# Activity of the yeast cytoplasmic Hsp70 nucleotide-exchange factor Fes1 is regulated by reversible methionine oxidation

Received for publication, July 9, 2019, and in revised form, December 2, 2019 Published, Papers in Press, December 5, 2019, DOI 10.1074/jbc.RA119.010125

Erin E. Nicklow and Carolyn S. Sevier[1]

*From the Department of Molecular Medicine, Cornell University, Ithaca, New York 14853*

Edited by Ruma Banerjee

**Cells employ a vast network of regulatory pathways to manage intracellular levels of reactive oxygen species (ROS). An effectual means used by cells to control these regulatory systems are sulfur-based redox switches, which consist of protein cysteine or methionine residues that become transiently oxidized when intracellular ROS levels increase. Here, we describe a methionine-based oxidation event involving the yeast cytoplasmic Hsp70 co-chaperone Fes1. We show that Fes1 undergoes reversible methionine oxidation during excessively-oxidizing cellular conditions, and we map the site of this oxidation to a cluster of three methionine residues in the Fes1 core domain. Making use of recombinant proteins and a variety of *in vitro* assays, we establish that oxidation inhibits Fes1 activity and, correspondingly, alters Hsp70 activity. Moreover, we demonstrate *in vitro* and in cells that Fes1 oxidation is reversible and is regulated by the cytoplasmic methionine sulfoxide reductase Mxr1 (MsrA) and a previously unidentified cytoplasmic pool of the reductase Mxr2 (MsrB). We speculate that inactivation of Fes1 activity during excessively-oxidizing conditions may help maintain protein-folding homeostasis in a suboptimal cellular folding environment. The characterization of Fes1 oxidation during cellular stress provides a new perspective as to how the activities of the cytoplasmic Hsp70 chaperones may be attuned by fluctuations in cellular ROS levels and provides further insight into how cells use methionine-based redox switches to sense and respond to oxidative stress.**

Oxidative stress is associated with an intracellular accumulation of high levels of reactive oxygen species (ROS).[2] ROS are widely appreciated as damage-inducing agents, based on their potential to irreversibly oxidize biological macromolecules, including lipids, nucleic acids, and proteins. Macromolecule oxidation as a consequence of excessive levels of cellular ROS can lead to a loss of vital cell functions and a deterioration of essential cellular processes. Historically, it has been generally accepted that decreasing or detoxifying ROS is key to limiting the cellular damage associated with oxidative stress. However, more recently, ROS have emerged also as signaling molecules, which can help cells initiate scavenging, protection, and repair pathways during oxidative stress (1). This conceptual shift suggests that preserving cell function during oxidative stress likely depends both on limiting ROS-induced damage and maintaining beneficial signaling events mediated by ROS.

Many of the identified ROS-based signaling pathways employ the use of labile, reversible redox-active post-translational protein modifications (PTMs) (2–7). Akin to the more established PTM phosphorylation, protein oxidation can reversibly alter the conformation and/or activity of a given protein. Altered protein activity can allow for the initiation of distinct downstream signaling events to benefit cells during oxidative stress, including the activation of pathways that serve to scavenge ROS before they exert detrimental effects as well as systems that act to manage and/or repair ROS-incurred damage (2–7).

Reversible oxidation of methionine side chains is one example of a redox-based PTM that can elicit beneficial cellular outcomes during oxidative stress (8, 9). Methionine modification by ROS occurs upon oxidation of the sulfur atom in the methionine side chain; addition of an oxygen molecule (from the ROS) to the sulfur generates a structure termed methionine sulfoxide (MetO). In eukaryotic cells, MetO adducts are reduced (reversed) by methionine sulfoxide reductase (Msr) enzymes (10). Advances in mass spectrometry (MS) and chemical biology tools have led to the identification of many proteins with methionine residues that are susceptible to oxidation (11, 12). Yet relative to other post-translational modifications, we are just beginning to uncover the impact of methionine oxidation on the function of individual proteins. Determining how oxidation influences protein function is an essential first step to reveal how modification may affect cell function during oxidative stress conditions.

Here, we report the susceptibility of, and consequences for, oxidation of three methionine residues in the yeast Hsp70 nucleotide-exchange factor (NEF) Fes1. Members of the heat-shock protein 70 (Hsp70) class of molecular chaperones play critical roles in maintaining protein homeostasis during peri-

This work was supported by National Institutes of Health Grant R01 GM105958 and a Cornell Schwartz Research Fund Award (to C. S. S.) and a Cornell Presidential Life Science Fellowship and National Institutes of Health Training Grant T32 GM008500 (to E. E. N.). The authors declare that they have no conflicts of interest with the contents of this article. The content is solely the responsibility of the authors and does not necessarily represent the official views of the National Institutes of Health.

This article contains Figs. S1–S4, Tables S1 and S2, and supporting Refs. 1–10.

[1] To whom correspondence should be addressed. Tel.: 607-253-3657; E-mail: css224@cornell.edu.

[2] The abbreviations used are: ROS, reactive oxygen species; PTM, post-translational modification; CHP, cumene peroxide; RFP, red fluorescent protein; NBD, nucleotide-binding domain; SBD, substrate-binding domain; NEF, nucleotide-exchange factor; Mxr, yeast methionine sulfoxide reductase; BME, β-mercaptoethanol; PMSF, phenylmethylsulfonyl fluoride; MetO, methionine sulfoxide; Msr, methionine sulfoxide reductase; NaOCl, sodium hypochlorite; tBHP, *tert*-butyl-hydroperoxide; ox, oxidized; HSR, heat-shock response; Trx1, thioredoxin; Trr1, thioredoxin reductase; FAM, 6-carboxyfluorescein; cv, column volume; dansyl, 5-dimethylaminonaphthalene-1-sulfonyl; Ni-NTA, nickel-nitrilotriacetic acid.; MABA-ADP, $N^8$-(4-*N*′-methylanthraniloylaminobutyl)-ADP.

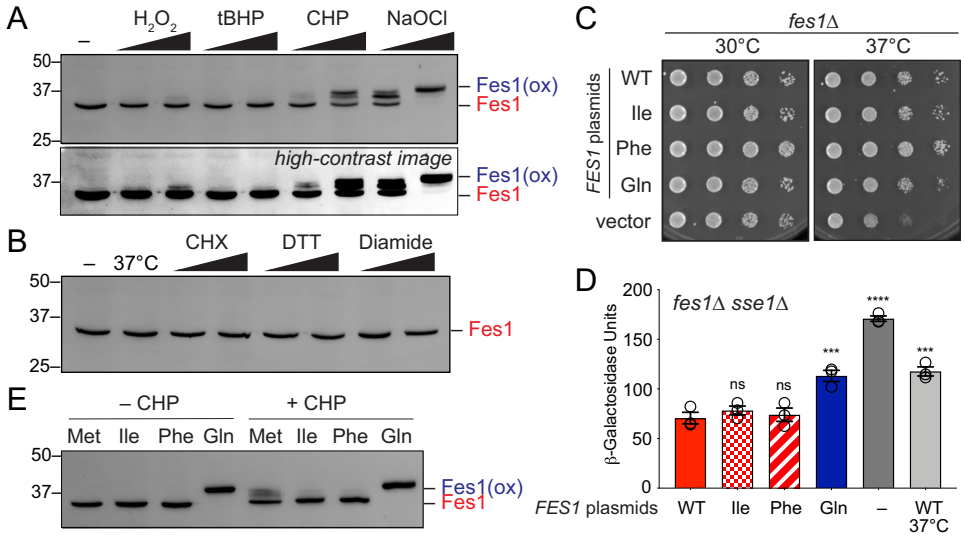


**Figure 1. Oxidation of Fes1 methionines occurs in cells exposed to exogenous ROS.** Lysates were prepared from WT yeast containing a plasmid encoding Fes1–FLAG after a 30-min treatment with peroxide (5 or 10 mM) or NaOCl (0.5 or 1 mM) (*A*) or after exposure to elevated heat (37 °C, 1 h), cycloheximide (*CHX*) (10 or 50 $\mu$g/ml, 30 min), DTT (5 or 10 mM, 30 min), or diamide (5 or 10 mM, 30 min) (*B*). Lysate proteins were separated by SDS-PAGE, and Fes1 was detected by Western blotting with anti-FLAG antibody. Mobility-shifted Fes1 corresponds to oxidized protein (see text). *C*, Fes1 methionine mutants complement temperature-sensitive growth of a *fes1*Δ strain. Yeast (*fes1*Δ cells) containing CEN plasmids encoding WT or methionine mutant Fes1–FLAG alleles were spotted onto selective synthetic minimal medium and assayed for growth at 30 or 37 °C for 2 days. *D*, suppression of the elevated *fes1*Δ cellular heat-shock response by Fes1 methionine mutant alleles. Cells (*fes1*Δ) containing plasmids encoding WT or methionine mutant Fes1–FLAG alleles and an HSE-*lacZ* reporter were cultured at 30 °C to log phase in minimal medium, and cultures were either maintained at 30 °C or shifted to 37 °C for 1 h. Three independent transformants of each strain were grown and assayed in duplicate. *Data points* represent the averaged values for the three independent transformants. *Bars* show the averaged values for the three transformants ± S.E. ****, $p \leq 0.0001$; ***, $p \leq 0.001$; $p \geq 0.05$ is defined as not significant (*ns*) by one-way analysis of variance, relative to the WT Fes1 expressing strain. *E*, lysates were prepared from a WT yeast strain containing the indicated Fes1–FLAG-expressing plasmids after treatment (or mock treatment) with 5 mM cumene hydroperoxide (CHP) for 30 min. Fes1 was detected by Western blotting with anti-FLAG antibody. Western images are representative of the data obtained from three independent experiments.

ods of oxidative stress. Extensive biochemical and biophysical studies have revealed a clear and conserved catalytic mechanism shared by the Hsp70 family (13–15). These prior studies establish that Hsp70s consist of two functional domains: a nucleotide-binding domain (NBD), which binds and hydrolyzes ATP, and a substrate-binding domain (SBD), which associates with peptide substrates. Hsp70 chaperone activity is facilitated by the binding and hydrolysis of ATP within the NBD, which promotes iterative cycles of peptide binding and release by the SBD. The intrinsic rate of Hsp70 ATP hydrolysis is low, and in cells, ATP turnover is facilitated by co-chaperones, including J-domain–containing proteins (which stimulate ATP hydrolysis) (16–18) and NEFs (which facilitate the exchange of ADP for ATP) (19, 20). The *Saccharomyces cerevisiae* protein Fes1 (HspBP1 in mammals) belongs to one of the three classes of cytosolic NEFs used by budding yeast to stimulate nucleotide exchange for the cytosolic Ssa and Ssb Hsp70s (21–24). Based on structural data for the Fes1 ortholog HspBP1, a mechanism for Fes1 NEF activity is proposed, wherein the C-terminal core region (that adopts series of Armadillo repeats) complexes with the Hsp70 NBD to mediate a conformational change in the NBD and ADP release (25). Fes1 additionally can help clear aggregation-prone peptides from the Hsp70 SBD through the action of its N-terminal region, which is predicted to be largely unstructured (26).

Here, we establish that Fes1 undergoes post-translational methionine sulfoxide modification during oxidative stress. We show that Fes1 oxidation is reversible and is mediated by cytosolic pools of the two yeast Msr enzymes: Mxr1 and Mxr2. We demonstrate that MetO modification diminishes the interaction between Fes1 and Hsp70, lessening the capacity for Fes1 to influence Hsp70 nucleotide exchange, peptide binding, and peptide release. We speculate that altering Hsp70 activities, as a consequence of Fes1 modification during stress, may help cells cope with elevated ROS by limiting peptide aggregation and/or activating cellular stress-response pathways.

## Results

### *Fes1 is post-translationally modified in cells by ROS*

We observed a striking change in the electrophoretic migration of Fes1 when cell lysates were prepared from yeast exposed to ROS. The most prominent change in Fes1 electrophoretic mobility was seen upon treatment of cells with sodium hypochlorite (NaOCl), a strong oxidant, classified as both a ROS and reactive chloride species (Fig. 1*A*). The extent of the mobility change in Fes1 intensified as the concentration of NaOCl in the medium was increased. Treatment with 0.5 mM NaOCl for 30 min resulted in several slower migrating Fes1 species (compared with untreated cells), and a single slow-migrating band was recovered in the presence of 1 mM NaOCl (Fig. 1*A*). Treatment of cells with a range of peroxides also resulted in changes to Fes1 mobility. Treatment with the organic peroxide cumene peroxide (CHP) caused a clear change in Fes1 migration; a striking shift was observed upon exposure of cells to 10 mM CHP for 30 min (Fig. 1*A*). In addition, a weaker but reproducible shift in Fes1 migration was observed upon addition of 10 mM hydrogen peroxide for 30 min (Fig. 1*A*). The same concentrations of *tert-*

**Table 1**

**Fes1 methionine-containing peptides identified by mass spectrometry**

Fes1 protein was immunoisolated from yeast cells grown in the absence or presence of peroxide, and Fes1 peptides were analyzed by mass spectrometry. Matched peptides containing five of the Fes1 methionines were recovered from both the untreated and treated samples. Methionines were identified in the reduced state (red), oxidized to methionine sulfoxide (diox), and oxidized to methionine sulfone (diox). ND, peptide not detected.

| Fes1 Met # | Peptide Fragment | Relative Abundance – CHP | Relative Abundance + CHP | Fold Enrichment |
|---|---|---|---|---|
| Met19 | LLQWSIANSQGDKEAM(red)AR | 1.00 | 1.00 | 1.00 |
| | LLQWSIANSQGDKEAM(ox)AR | 1.92 | 3.28 | 1.71 |
| | LLQWSIANSQGDKEAM(diox)AR | ND | ND | – |
| Met45 | LLQQLFGGGGPDDPTLM(red)K | 1.00 | 1.00 | 1.00 |
| | LLQQLFGGGGPDDPTLM(ox)K | 5.18 | 6.11 | 1.18 |
| | LLQQLFGGGGPDDPTLM(diox)K | 0.06 | 0.12 | 2.00 |
| Met49 / Met53 | ESM(red)AVIM(red)NPEVDLETK | 1.00 | 1.00 | 1.00 |
| | ESM(ox)AVIM(red)NPEVDLETK | 1.80 | 2.60 | 1.44 |
| | ESM(ox)AVIM(ox)NPEVDLETK | 5.80 | 18.83 | 3.25 |
| | ESM(diox)AVIM(ox)NPEVDLETK | 0.77 | 3.49 | 4.53 |
| Met79 | *Incomplete coverage* | | | |
| Met126 | AAALSIIGTAVQNNLDSQNNFM(red)K | 1.00 | 1.00 | 1.00 |
| | AAALSIIGTAVQNNLDSQNNFM(ox)K | 7.00 | 7.00 | 1.00 |
| | AAALSIIGTAVQNNLDSQNNFM(diox)K | 0.04 | 0.05 | 1.25 |
| Met194 | *Incomplete coverage* | | | |

butyl-hydroperoxide (tBHP) did not result in a detectable change in Fes1 migration (Fig. 1*A*), although even higher concentrations of tBHP were found to induce mobility changes (data not shown). The relative sensitivity of Fes1 to the distinct peroxides is in keeping with the relative yeast toxicity reported for these peroxides; a <10% survival has been established for 4 mM CHP, 6 mM hydrogen peroxide, and 15 mM tBHP, respectively (27, 28). Although exposure to several types of ROS resulted in a clear migration change in Fes1, exposure to other common stressors did not alter Fes1 mobility on SDS-PAGE. Yeast that underwent heat shock, treatment with cycloheximide (CHX), exposure to the reductant (DTT), or incubation with the thiol-oxidant diamide yielded no change in Fes1 mobility (Fig. 1*B*).

The mobility change we observed for Fes1 was suggestive of a post-translational protein modification triggered by ROS exposure. Prior studies have demonstrated that oxidation of protein methionine residues can cause a pronounced change in protein migration through a reducing SDS-polyacrylamide gel (29–31). We reasoned that the shift in Fes1 mobility could be a consequence of methionine oxidation induced by ROS exposure. To monitor whether Fes1 methionine residues are oxidized in cells exposed to exogenous ROS, we used MS to analyze peptides from Fes1 immunoisolated from untreated yeast cells or from cells exposed to 10 mM CHP for 30 min. It is established that methionine oxidation can be induced at several steps during sample preparation for MS analysis (32–34), and care was taken to minimize methionine oxidation post-cell lysis (see "Experimental procedures"). Fes1 contains seven methionines distributed throughout the protein; matched peptides for five of the seven methionines were recovered and identified by ESI-LC-MS/MS from both the untreated and treated samples. Methionines in peptides from stressed and unstressed cells were identified in the reduced state (Met; red) and also oxidized to methionine sulfoxide (MetO; ox) or methionine sulfone ($MetO_2$; diox) (Table 1). Some methionine oxidation was detected at all five methionines in both the CHP-treated and -untreated samples (Table 1). Although we cannot exclude the possibility that Fes1 methionine oxidation occurs in cells under basal growth conditions, we think it is likely given the numerous reports on artificial oxidation during the MS workflow that sample preparation induced some (or most) of the Fes1 oxidation observed in the unstressed samples. Closer analysis of the MS data revealed four methionine residues in Fes1 (Met-19, Met-45, Met-49, and Met-53) showed increased oxidation levels in the protein isolated from peroxide-treated cells (Table 1). These four methionines appeared selectively susceptible to oxidation; an enrichment in oxidation was not observed for Fes1

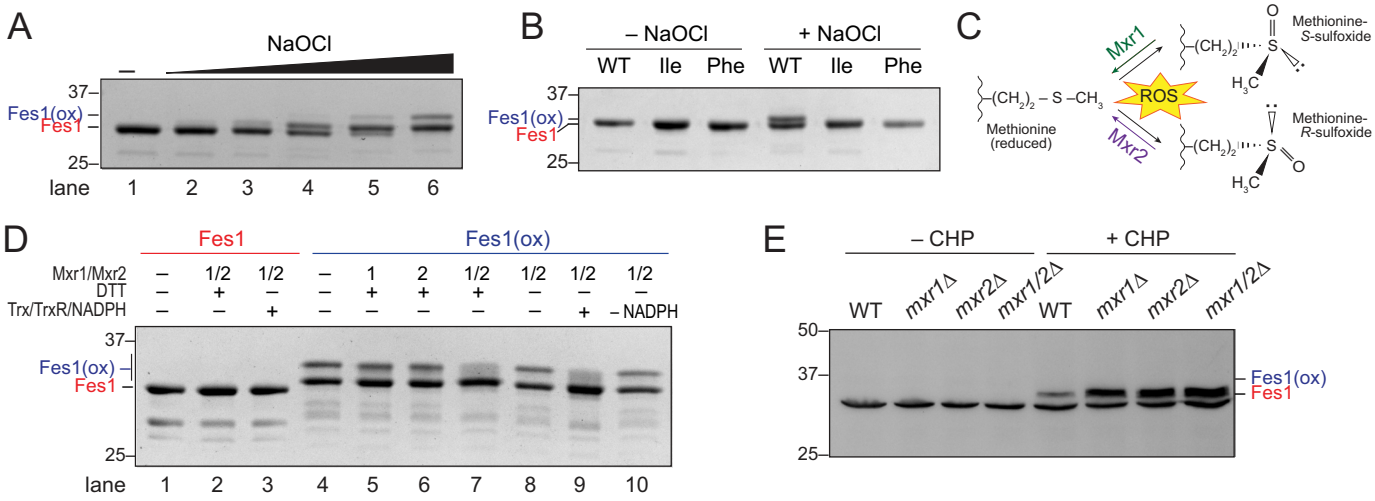


**Figure 2. Oxidation of Fes1 is reversed by both *R*- and *S*-type methionine sulfoxide reductases.** *A,* electrophoretic mobility shifts are observed when recombinant Fes1 protein is treated with NaOCl at increasing concentrations (0–20-fold molar excess). *B*, purified recombinant Fes1 methionine mutants are resistant to oxidation. Fes1 protein with Met residues 45, 49, and 53 mutated to Ile or Phe were treated with a 10-fold molar excess of NaOCl. Oxidation of Fes1 was assessed based on the change in mobility. Recombinant proteins were visualized with Coomassie Brilliant Blue after SDS-PAGE. *C*, methionine sulfoxide reductase enzymes catalyze the reduction of MetO in a stereospecific manner. In the presence of ROS, protein methionine residues can be modified to generate *S*- and *R*-MetO isomers; oxidized methionine stereoisomers are reduced in yeast by Mxr1 (reduces *S*-MetO) and Mxr2 (reduces *R*-MetO). *D*, Mxr1 and Mxr2 reduce oxidized Fes1. Fes1 protein was oxidized with NaOCl then treated with Mxr1 and Mxr2 alone (*lanes 5* and *6*) or in combination (*lanes 7–10*). To catalyze Mxr enzyme turnover, DTT or a reconstituted thioredoxin system (consisting of Trx1, Trr1, and NADPH) was used. Proteins were separated by SDS-PAGE and visualized by staining with Coomassie Brilliant Blue. *E,* methionine sulfoxide reductases modulate the redox state of Fes1 *in vivo*. Lysates were prepared from log-phase cultures of the indicated WT or *mxr*Δ yeast strains (containing a Fes1–FLAG plasmid) after treatment with 5 mM CHP for 30 min. Proteins were separated by SDS-PAGE, and Fes1 was detected by Western blotting with anti-FLAG antibody. Images shown are each representative of three independent experiments.

methionine Met-126 (Table 1). We were further struck by the increased relative abundance of peptides containing oxidized Met-45, Met-49, and Met-53 under basal conditions (5.2–5.8-fold relative to reduced peptides), which was further increased upon peroxide treatment (Table 1). We suggest that increased oxidation of a given methionine during sample preparation may also indicate a methionine residue particularly prone to modification, especially when recovery of the same oxidized methionine is further noted in peroxide-treated samples. The three Fes1 methionines that attracted our attention (Met-45, Met-49, and Met-53) cluster within the area of sequence predicted to localize to the first $\alpha$-helix ($\alpha$1) of the Fes1 core domain (Fig. S1).

To determine whether oxidation of methionines 45, 49, and 53 accounts for the slower mobility of Fes1 observed upon peroxide treatment (Fig. 1*A*), we generated alleles of Fes1 with Met-45, Met-49, and Met-53 mutated to the somewhat structurally similar residues isoleucine and phenylalanine, and to glutamic acid. Mutation of the three methionines resulted in Fes1 protein that retained *in vivo* activity. Yeast cells lacking a functional copy of *FES1* (a *fes1*Δ strain) show decreased growth at elevated temperatures, compared with WT cells (21, 35, 36). Expression of a Fes1 Met–to–Ile, Met–to–Phe, or Met–to–Gln triple mutant in the *fes1*Δ background restored growth to similar levels as expression of WT Fes1 (Fig. 1*C*). It has been shown that a double deletion strain lacking two of the cytoplasmic yeast NEFs (a *fes1*Δ *sse1*Δ strain) shows a strongly up-regulated heat-shock response (HSR) (21). Expression of a Fes1 Met–to–Ile or a Met–to–Phe triple mutant was found to dampen the HSR in a *fes1*Δ *sse1*Δ strain, similar to the decrease in HSR observed with addition of a WT Fes1 encoding plasmid (Fig. 1*D*). Despite rescuing the high-temperature growth defect, a Fes1 Met–to–Gln mutant showed only a partial down-regulation of the heat-shock response, relative to a *fes1*Δ *sse1*Δ strain (Fig. 1*D*), and we suggest that this mutant may be partially compromised for Fes1 activity. Importantly, consistent with the MS data, we found that the electrophoretic mobility of a Fes1 Met–to–Ile, Met–to–Phe, or Met–to–Gln triple mutant did not change when cells were exposed to CHP (Fig. 1*E*), supporting the conclusion that the Fes1 size shift induced by oxidant exposure is a consequence of methionine oxidation at residues Met-45, Met-49, and Met-53. A Fes1 Met–to–Gln triplet mutant showed a slower electrophoretic mobility (similar to that observed for oxidized WT Fes1) in both untreated and oxidant-treated cells, which is likely a consequence of the negative charge associated with the glutamine side chain. Similarities between protein methionine sulfoxide and glutamine have been previously described (37, 38), and we speculate that the Met–to–Gln allele could be mimicking (in part) the oxidized form (see under "Discussion").

### *Oxidative modification of Fes1 is reversed by R- and S-type methionine sulfoxide reductases*

Protein methionines oxidized to methionine sulfoxide (MetO) can be reversed by methionine sulfoxide reductase (Msr) enzymes (39). To determine whether the activity of the yeast Msrs could reverse oxidation of Fes1, we established a cell-free assay to monitor Fes1 oxidation. Recombinant Fes1 was purified from bacteria and treated with NaOCl. Similar to what was observed in cells, we saw a clear change in Fes1 mobility when protein was incubated with increasing concentrations of oxidant (Fig. 2*A*). Modest changes in mobility were observed even the presence of an equimolar concentration of NaOCl (Fig. 2*A*, *lane 2*). When Fes1 was treated with a 10-fold (or

higher) molar excess of NaOCl, there was very little, or a complete absence, of any Fes1 species co-migrating with untreated (reduced) Fes1 (Fig. 2*A*, *lanes 5* and *6*). Recombinant Fes1 Met–to–Ile and Met–to–Phe triple mutants did not undergo a mobility change in the presence of oxidant, establishing that the same Fes1 methionines oxidized in cells are susceptible to modification *in vitro* (Fig. 2*B*).

Yeast encode two Msr enzymes (Mxr1 and Mxr2) that reduce protein-incorporated MetO modifications in a stereospecific manner. Yeast Mxr1 (MsrA) and Mxr2 (MsrB) have been linked to the reduction of protein *S*-MetO and *R*-MetO, respectively (Fig. 2*C*) (40). We purified recombinant versions of Mxr1 and Mxr2 and set up an *in vitro* system to monitor activity toward oxidant-treated Fes1. Recombinant Fes1 protein was oxidized with NaOCl and then incubated with substoichiometric amounts (a 1–to–10 ratio of Mxr–to–Fes1) of Mxr1 and Mxr2, either alone (Fig. 2*D*, *lanes 5* and *6*) or in combination (Fig. 2*D*, *lanes 7–10*). To catalyze multiple reaction turnovers, DTT or a reconstituted yeast thioredoxin system (consisting of thioredoxin (Trx1), thioredoxin reductase (Trr1), and NADPH) was provided to recycle (reduce) the Msrs. Note, the presence of DTT alone is insufficient to reduce protein–MetO adducts. We observed a clear loss of the slowest migrating, oxidant-induced Fes1 band in the presence of both Msr enzymes and a recycling system (Fig. 2*D*, *lanes 7* and *9*). Both the thioredoxin and DTT recycling systems yielded a similar reduction in the slower-migrating Fes1 species (Fig. 2*D*). Incubation of Fes1 in the presence of a single Msr led to a very modest decrease in the more slowly migrating oxidized Fes1 species (Fig. 2*D*, *lanes 5* and *6 versus 4*), and we hypothesize that the synergistic effect of Mxr1 and Mxr2 results from their combined ability to reduce the anticipated mixtures of *R*- and *S*-MetO Fes1 species. Of note, a complete restoration of a band that co-migrates with reduced Fes1 was not obtained, and we speculate that some portion of the *in vitro*-modified Fes1 contains methionines oxidized to methionine sulfone ($MetO_2$), which is resistant to reduction by Msrs. Such an overoxidation of protein methionines in the cell-free system is not unexpected, given the 10-fold excess of oxidant used to oxidize Fes1 in the absence of any cellular system that may serve to limit overoxidation. In addition, we cannot eliminate the possibility that Fes1 is oxidized also at nonmethionine residues, which would not be reversed by Msr activity; however, the oxidant-treated Fes1 methionine mutants did not show a shift in size upon oxidant treatment (Fig. 2*B*), suggesting that the remaining size-shifted species in the Msr-treated oxidized Fes1 samples (Fig. 2*D*) reflect methionine modification. Altogether, these data confirm that the migration change for Fes1 induced in the presence of oxidant is a by-product of methionine oxidation, which can be reversed (in part) through the activity of the yeast Msr enzymes Mxr1 and Mxr2.

Given the ability of recombinant Mxr1 and Mxr2 to reverse Fes1 oxidation *in vitro*, we next sought to establish the ability of either or both enzyme(s) to modulate Fes1 oxidation *in vivo*. We reasoned that if the Msr enzymes mediate reduction of Fes1 in cells, yeast strains lacking Msr activity would accumulate more oxidized Fes1 protein. In keeping with our expectation, we observed yeast deleted for either Msr enzyme (*mxr1*Δ or *mxr2*Δ) and treated with peroxide showed an increased level of Fes1 oxidation, compared with WT cells treated with the same concentration of oxidant (Fig. 2*E*). In contrast to our *in vitro* experiments, we did not see a clear combinatorial effect for a loss of both Mxr enzymes on Fes1 oxidation; an *mxr1*Δ *mxr2*Δ double deletion strain showed no further increase in oxidized Fes1 levels compared with the single mutant strains (Fig. 2*E*). Although we expected a loss of both enzymes would yield a further increase in the accumulation of oxidized Fes1, due to their distinct activities toward MetO isomers, we speculate that the observed yeast phenotype could reflect compensatory yeast systems that allow for the growth and viability of the double mutant strain.

### *Cytoplasmic pool of Mxr2 influences Fes1 oxidation*

Previous studies have localized yeast Mxr1 to the cytoplasm and Mxr2 within the mitochondria (40, 41), and thus we were initially surprised to observe an impact for loss of Mxr2 activity on the oxidation of cytoplasmic Fes1. Although the impact for loss of Mxr2 on cellular Fes1 oxidation could be indirect, we were intrigued by the alternative possibility that an uncharacterized cytoplasmic pool of Mxr2 may exist that could directly reduce Fes1, as observed in our *in vitro* system. Mining the compiled ribosome-profiling and mRNA-sequencing database (42) revealed the potential for prominent use of an internal methionine start codon in Mxr2 (Met-34), numbered relative to the annotated start site (Met-1) (Fig. S2). We hypothesized that translation initiated from Met-34 would generate a protein with an intact enzymatic core that would lack the amphipathic mitochondrial targeting sequence encoded by residues 1–30 (43). We speculated that an Mxr2 protein translated from Met-34 would be localized to the cytoplasmic space, where it could facilitate reduction of oxidized proteins. A similar binary start-site mechanism has been described for other proteins dual-localized to the cytosol and mitochondria (44).

To determine the subcellular distribution of Mxr1 and Mxr2 in yeast, we fractionated lysates prepared from cells expressing GFP-tagged Mxr1 or Mxr2 proteins. Lysates were separated into mitochondrial and cytosolic fractions, and proteins in each fraction were probed for Mxr1/2 (using anti-GFP serum) or for established mitochondrial (porin; Por1/2) and cytosolic (phosphoglycerate kinase; Pgk1) proteins, to confirm the separation of the mitochondrial and cytoplasmic protein pools (Fig. 3*A*). Consistent with prior reports, Mxr1 fractionated with the cytosolic marker Pgk1 (Fig. 3*A*) (40). Some Mxr1 and Pgk1 signals were detected in the mitochondrial fraction (Fig. 3*A*); given the established localization of Pgk1 in the cytoplasm, we speculate that the mitochondrial signal for these proteins is a consequence of carryover from the cytosolic fractions during the experimental protocol. Strikingly, the Mxr2 protein also appeared predominantly in the cytosolic fraction (Fig. 3*A*); no signal for Mxr2 was detected in the mitochondrial fraction. We cannot rule out that a lower level of mitochondrial Mxr2 protein exists in addition to the cytosolic pool and that this mitochondrial Mxr2 protein pool is below the limit of detection of our assay. Yet, overall our data suggest a predominant cytosolic localization for both Mxr1 and Mxr2. To link the presence of a cytosolic Mxr2 pool and the potential use of an internal (Met-34) start codon, we next mutated the two potential start sites in

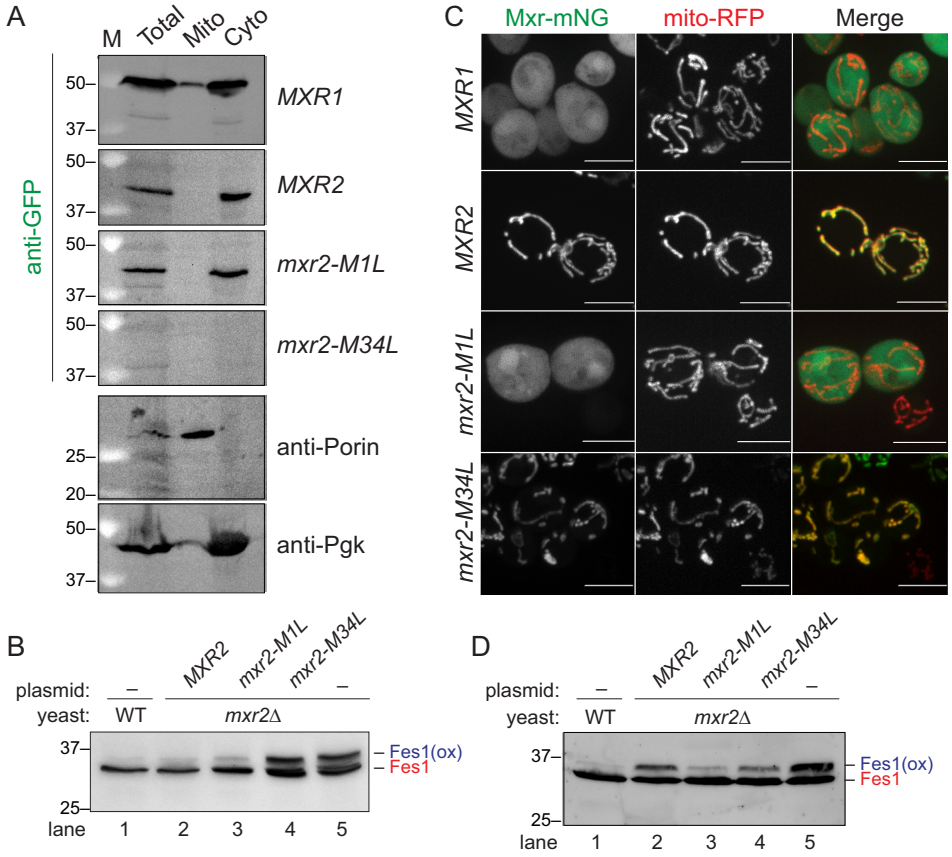


**Figure 3. Cytosolic pool of Mxr2 influences Fes1 oxidation.** *A,* post-nuclear lysate from WT yeast cells expressing GFP-tagged Mxr proteins under the control of the endogenous *MXR* promoters were subject to differential centrifugation to separate mitochondria (*Mito*) from the cytosolic (*Cyto*) fraction. Fractionated protein samples were separated by SDS-PAGE, and Mxr proteins were detected by Western blotting with anti-GFP antibody. Phosphoglycerate kinase (*Pgk*) and Porin were used as markers of the cytosolic and mitochondrial fractions, respectively, and these proteins were detected with the indicated antibodies. *B,* plasmids encoding WT or the indicated mutant alleles of Mxr2 (untagged and under control of the endogenous *MXR2* promoter) were transformed into an *mxr2*Δ strain that contained a plasmid-borne copy of Fes1–FLAG. Yeast were cultured to log phase and treated with 5 mM CHP for 30 min prior to harvest. Lysate proteins were separated by SDS-PAGE, and Fes1 was detected by Western blotting with anti-FLAG antibody. *C,* WT yeast expressing plasmid-borne Mxr constructs, tagged with mNeonGreen, under the control of a *TEF2* promoter were imaged by confocal fluorescence microscopy. A mitochondrial-targeted RFP serves as a mitochondrial marker. *Scale bar* indicates 5 μm. *D,* plasmids encoding WT or the indicated mutant alleles of Mxr2 (tagged with mNeonGreen and under the control of the *TEF2* promoter) were transformed into an *mxr2*Δ strain containing a plasmid-borne copy of Fes1–FLAG. Yeast cells were grown and treated with peroxide, and lysate protein samples were processed as described in *B*.

Mxr2, generating Met–to–Leu substitution alleles at Mxr2 Met-1 and Met-34. An Mxr2 lacking the annotated Met-1 start codon (Mxr2–M1L) resulted in a cytosolic localization for Mxr2, which appeared unchanged from the expression level and localization of WT Mxr2 (Fig. 3*A*). These data suggest the cytosolic pool is generated by initiation at a methionine other than the annotated Met-1 start site. In contrast, signal from an Mxr2–M34L protein was not detected in any cellular fractions (Fig. 3*A*). Although it is possible that the lack of detectable Mxr2–M34L expression arises from instability (and subsequent turnover) of a mutant protein (initiated at Met-1), we suggest this result indicates Met-34 is the predominant start codon for Mxr2 translation in cells. Indeed, use of Met-34 as a primary start site is supported by data from the compiled ribosome-profiling database, which reveals minimal footprints for both scanning and elongating ribosomes at the Met-1 site compared with Met-34 (Fig. S2).

To determine whether the cytosolic Mxr2 modulates Fes1 oxidation, we took advantage of the increase in Fes1 oxidation observed in an *mxr2*Δ strain treated with peroxide (Figs. 2*E* and 3*B*, *lane 5*). We confirmed first that addition of a plasmid encoding WT Mxr2 could rescue the increased Fes1 oxidation phenotype of the *mxr2*Δ strain; we established that the presence of a *MXR2* plasmid resulted in less Fes1 oxidation upon peroxide treatment (Fig. 3*B*, *lane 2*) similar to what was observed in a WT yeast strain (Fig. 3*B*, *lane 1*). Addition of a plasmid encoding Mxr2–M1L protein resulted in a similar outcome as observed for a plasmid encoding WT Mxr2 (Fig. 3*B*, *lane 3*), suggesting that a cytoplasmic pool of Mxr2 (initiated at a start site distinct from Met-1) accounts for the relative decrease in accumulated Fes1 oxidation in a WT strain *versus* an *mxr2*Δ. A strain containing a plasmid coding for Mxr2–M34L accumulated higher levels of oxidized Fes1 (Fig. 3*B*, *lane 4*), analogous to the levels in an *mxr2*Δ strain. The absence of detectable, tagged Mxr2–M34L protein (Fig. 3*A*) leads us to suggest that the absence of Fes1 MetO-reduction activity in this stain is a consequence of no (or low levels of) functional Mxr2 protein.

Our results indicate an underappreciated cytoplasmic pool of Mxr2 that can influence the level of oxidized Fes1; these results contrast with prior reports of a sole mitochondrial localization for Mxr2 (40, 41). A distinction between our experi-

ments and these previous studies is our use of constructs wherein Mxr2 expression is controlled by the endogenous *MXR2* promoter; prior localization of Mxr2 to the mitochondria was established using constructs with stronger, nonnative promoters to drive Mxr2 expression: *GAL* (40) or *TEF* (41). Notably, in each case, this strong promoter was fused proximal to the Met-1 codon sequence; correspondingly, the Met-34 codon would be more distant in sequence (~100 bp) from the nonnative promoter sequence. To follow localization of Mxr2 under similar conditions as those previously reported, we generated C-terminally–tagged mNeonGreen Mxr constructs under control of the *TEF2* promoter. We assessed the localization of these proteins using fluorescence confocal microscopy (Fig. 3*C*). Under these conditions, Mxr1 showed a diffuse fluorescence distribution throughout the cell (Fig. 3*C*); the cytoplasmic localization of Mxr1 was consistent both with previous studies (40) and also the localization we observed for Mxr1 expressed from its endogenous promoter (Fig. 3*A*). Importantly, we observed that the *TEF*-promoted Mxr2 co-localized with the mitochondria, visualized by a mitochondrial-targeted RFP (Fig. 3*C*). Substitution of Met-34 had no impact on localization of the *TEF*-promoted Mxr2; the Mxr2–M34L proteins localized to the mitochondria similar to WT Mxr2 (Fig. 3*C*). In contrast, an Mxr2–M1L protein resulted in a cytoplasmic localization for Mxr2 (Fig. 3*C*), suggesting that use of an internal start methionine allows for generation of a cytoplasmic form of Mxr2 (in the absence of Met-1). Altogether, we conclude that a mitochondria-localized Mxr2 protein is translated when the annotated open reading frame (ORF) is juxtaposed with a strong promoter. Yet, our data suggest that when translation is mediated by endogenous sequences surrounding the annotated ORF, translation preferentially starts at an internal methionine. We suggest that this internal methionine is Met-34; in support of this conclusion, mutation of Met-34 to Leu, in a construct containing the native 5′ UTR, results in no detectable Mxr2 protein (Fig. 3*A*).

To determine whether the subcellular localization of Mxr2 influences its ability to modulate Fes1 oxidation, we took advantage of the distinct intracellular distribution of the *TEF*-promoted WT and mutant Mxr2 proteins (Fig. 3*C*). We observed that the predominantly cytoplasmic Mxr2 (Mxr2–M1L) was most efficient at limiting the accumulation of oxidized Fes1 in peroxide-treated cells (Fig. 3*D*, *lane 3*). In contrast, more oxidized Fes1 accumulated in peroxide-treated cells containing the mitochondria-localized Mxr2 and Mxr2–M34L proteins (Fig. 3*D*, *lanes 2* and *4*). Of interest, the strain expressing *TEF*-promoted Mxr2 showed higher levels of oxidized Fes1 than a WT strain (Fig. 3*D*, *lane 2 versus 1*), suggesting that overexpression of Mxr2 from a nonnative promoter results in less reduction of Fes1 than observed in a strain containing a lower level of Mxr2 expression mediated by its endogenous promoter. We speculate that endogenous Mxr2, present in the cytoplasm of a WT strain, is able to reduce cytoplasmic Fes1, whereas a mitochondrial pool of Mxr2 (driven by the nonnative promoter) is not sufficient to fully rescue the observed elevated levels of Fes1 oxidation in an *mxr2*Δ strain.

Our data suggest the potential for both cytoplasmic and mitochondrial Mxr2 forms that modulate MetO oxidation of protein substrates within these respective compartments. Such a cross-organelle distribution would be consistent with the reported multiple isoforms of the mammalian methionine sulfoxide reductase MsrB, which are localized to multiple intracellular compartments, including the cytosol, mitochondria, nucleus, and endoplasmic reticulum (45).

### *Fes1 oxidation alters its ability to modulate Hsp70 activities*

Having established the susceptibility of Fes1 to methionine oxidation, we next sought to determine how oxidation impacts the established abilities of Fes1 to facilitate Hsp70 nucleotide exchange and substrate release (Fig. 4*A*) (22, 24, 26, 35).

To monitor NEF activity, we employed stopped-flow spectroscopy and the fluorescent ADP analog MABA-ADP. When bound to Hsp70, MABA-ADP shows enhanced fluorescence; nucleotide release from the Hsp70 manifests as a decrease in fluorescence (46, 47). Yeast contain two classes of cytoplasmic Hsp70s, grouped based on sequence homology: the Ssa and Ssb proteins (48). Prior reports have demonstrated that Fes1 shows a similar affinity toward Ssa1 and Ssb1 (22) and that Fes1 is effective as an Ssa1 and Ssb1 NEF (22, 24). A majority of published reports focus on Ssa1 as the model cytoplasmic Hsp70, and we continue this trend for most of our biochemical assays. However, we found that the Ssa1 protein purified with bound nucleotide, which we were unable to effectively remove (see "Experimental procedures"). Thus, for the NEF assays we made use of recombinant Ssb1 protein, which in its apo-state could be efficiently loaded with MABA-ADP. Complexes were formed between recombinant Ssb1 and MABA-ADP. Release of MABA-ADP from Ssb1 (in the presence of an excess of unlabeled ADP) was found to be relatively slow in the absence of a NEF (Fig. 4, *B* and *C*); an average MABA-ADP off-rate of $0.189 \pm 0.009\ s^{-1}$ was measured (Fig. 4*C*), which is similar to the previously reported rates of $0.205 \pm 0.001\ s^{-1}$ (22) and $0.27\ s^{-1}$ (24). Addition of Fes1 accelerated the rate of MABA-ADP release from Ssb1 ~9-fold, increasing the off-rate to $1.634 \pm 0.098\ s^{-1}$ (Fig. 4*C*). These data are consistent with the previously reported ability of Fes1 to stimulate MABA-ADP release from Ssb1 (22, 24).

To test the effect of Fes1 oxidation on its activity as a NEF, oxidized Fes1 was prepared by treating recombinant protein with a 10-fold molar excess of NaOCl. To prevent oxidation of Ssb1 protein, all the oxidant-treated Fes1 samples (and the oxidant-treated buffer control) were run through a desalting column prior to injection into the stopped-flow apparatus. Treatment with oxidant was observed to lessen Fes1 NEF activity (Fig. 4, *B* and *C*). The rate of Ssb1 nucleotide release stimulated by oxidized Fes1 was diminished ~4-fold relative to reduced Fes1, exhibiting an average measured off-rate for MABA-ADP of $0.404 \pm 0.083\ s^{-1}$. The inhibitory effect of oxidant treatment was partially reversible. Treatment of the desalted oxidized Fes1 protein with a mixture of Mxr1 and Mxr2, prior to mixing with Ssb1–MABA-ADP, resulted in a Fes1 protein that stimulates nucleotide release ~5-fold, relative to the rate observed in the absence of Fes1 (Fig. 4*C*). The partial restoration of Fes1 activity was consistent with the partial restoration in Fes1 mobility seen upon incubation with a combination of Mxr1 and Mxr2 (Fig. 2*D*). It is worth noting that we were unable to mon-

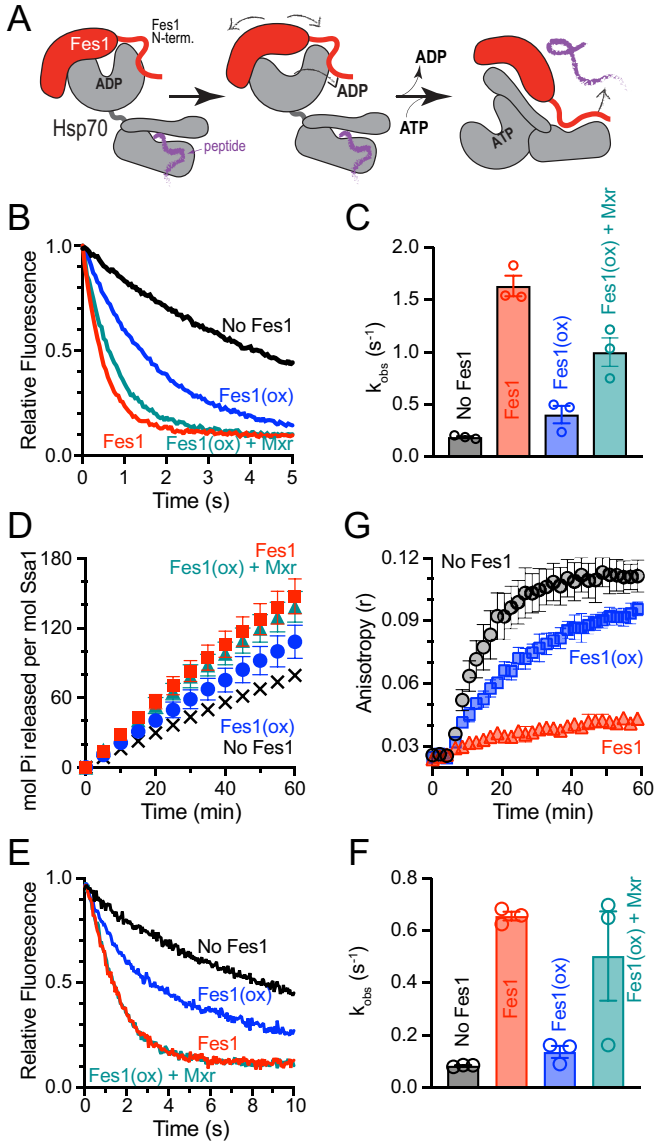


**Figure 4. Oxidation lessens Fes1 regulation of Hsp70 activities.** *A,* model for Fes1–Hsp70 interactions. Fes1 binds to an Hsp70–ADP–peptide complex and mediates the separation of the lobes of the Hsp70 NBD to facilitate ADP release. The association of ATP with apo-Hsp70 induces peptide release. The Fes1 core domain dissociates from ATP-bound Hsp70. The Fes1 N terminus can bind to the open Hsp70 substrate-binding pocket to prevent peptide re-association. *B* and *C,* ability of Fes1 to catalyze the exchange of nucleotide bound to Ssb1 was monitored by stopped-flow. Ssb1 preloaded with MABA-ADP was chased with an excess of ADP in the presence of untreated Fes1, oxidant-treated Fes1 (*Fes1(ox)*), or Fes1(ox) pre-incubated with Mxrs. Averaged fluorescence values, from a minimum of six replicates, are shown for one independent experiment in *B*. *C* shows the rates ± S.E. for three independent experiments, where the rates for each experiment were determined from the nonlinear fit of the average values from at least five technical replicates. *D,* Ssa1 ATPase activity was monitored by following the accumulation of free phosphate in the presence of the Ydj1 J-domain and Fes1. Data depict the average from three independent experiments. *Error bars* represent the S.E. *E* and *F,* release of bound NBD-labeled NR peptide from Hsp70 was monitored by stopped-flow. Hsp70 preloaded with peptide was chased with an excess of unlabeled NR peptide and ATP in the presence of Fes1, Fes1(ox), or Fes1(ox) pretreated with Mxrs. *E* shows the averaged fluorescence values of a minimum of six replicates from one independent experiment. *F* shows the rates from three experiments, determined from the nonlinear fit of the average data from at least five technical replicates per experiment. *Error bars* represent the S.E. *G,* ability of Fes1 to inhibit peptide association with Hsp70 was monitored by anisotropy. Hsp70, or preformed Hsp70–Fes1 complexes, were rapidly mixed with FAM–NR peptide, and data were collected over 1 h. Average anisotropy values from three independent experiments are shown ± S.E.

itor the activity of the Fes1 triple methionine mutants in the NEF assay. Based on our prior data (Fig. 2*B*), we expected that a Fes1 methionine mutant treated with oxidant would likely retain NEF activity. However, we found that the Met–to–Ile, Met–to–Phe, and Met–to–Gln mutants were compromised for NEF activity even in the absence of oxidant (Fig. S3). We suggest the lessened activity for these mutants reflects the biochemical importance of these methionine residues for Fes1 NEF activity, which is, in turn, altered upon modification of these residues either post-translationally (by oxidant) or through mutagenesis. We speculate that the lower NEF activity measured for the Met–to–Ile and Met–to–Phe mutants *in vitro* may be sufficient to complement the yeast phenotypes associated with a loss of cellular Fes1 activity (a *fes1*Δ) (Fig. 1, *C* and *D*). Alternatively, it was recently reported that a Fes1 mutant protein deficient for Hsp70 binding (Fes1–A79R-R195A) can complement some *fes1*Δ phenotypes in yeast, including the slower growth of a *fes1*Δ strain at high temperature (49). Thus, the ability of the Fes1 methionine triplet mutants to support growth comparable with WT Fes1 at elevated temperatures (Fig. 1*C*) may reflect an activity of Fes1 independent of its NEF activity.

We reasoned the lower NEF activity observed for oxidized Fes1 would translate to a decreased ability of oxidized Fes1 to stimulate Hsp70 ATPase activity. To monitor ATPase activity, we followed ATP hydrolysis by Ssa1 protein purified from yeast. Similar to the NEF activity assays, we observed that WT Fes1 stimulated ATP turnover by Ssa1 and that the stimulatory activity of Fes1 was decreased upon treatment of Fes1 with oxidant (Fig. 4*D*). The damped activity for oxidized Fes1 was reversed by treatment with Mxr1 and Mxr2 (Fig. 4*D*). Given the location of the oxidation-sensitive methionines in proximity to the N-terminal domain (Fig. S1), we speculated that the lack of activity observed for oxidized Fes1 might be mediated by changes to the N-terminal region. However, we observed that the presence of the N terminus is not necessary to mediate oxidant-induced changes to Fes1 activity (Fig. S4).

A consequence of stimulated Hsp70 nucleotide release by a cytoplasmic NEF is the association of Hsp70 with ATP, which facilitates peptide release (Fig. 4*A*) (22, 25, 50). The NR peptide (sequence: NRLLLTG) and a derivative of the APPY peptide (Ala-P5: ALLLSAPRR) have been shown to be substrates for the cytoplasmic Hsp70 Ssa1 (25, 50–52). Hence, to monitor the influence of Fes1 on peptide binding, we made use of the Ssa1 protein and an NR peptide labeled with the environmentally-sensitive fluorophore NBD, which shows enhanced fluorescence when in complex with an Hsp70. We initially planned to also monitor Ssb1–peptide interactions, but we were unable to detect an association of labeled peptide with Ssb1 (data not shown); a similar lack of detectable interaction between Ssb1 and APPY–peptide has been noted previously (51). Complexes of Ssa1 were formed with the NBD–NR peptide. Using stopped-flow spectroscopy, we monitored the ability of Fes1 to stimulate a decrease in NBD–NR fluorescence upon mixing of the Ssa1–NBD–NR complex with an excess of ATP and unlabeled peptide. In the absence of Fes1, we observed a peptide release off-rate of 0.083 ± 0.002 $s^{-1}$, which was accelerated ~8-fold by Fes1 ($k_{obs}$ of 0.66 ± 0.017 $s^{-1}$) (Fig. 4, *E* and *F*).

Oxidant-treated Fes1 showed a decreased ability to stimulate peptide release from Ssa1; relative to the off-rate observed in the presence of untreated Fes1, oxidant-treated Fes1 peptide release was slowed ~5-fold ($k_{obs}$ of 0.136 ± 0.023 $s^{-1}$) (Fig. 4, *E* and *F*). The activity of oxidant-treated Fes1 was restored when incubated with a combination of Mxr1 and Mxr2, resulting in an average off-rate for the Ssa1–peptide complex of 0.503 ± 0.17 $s^{-1}$ (Fig. 4*F*). Interestingly, peptide release kinetics appeared to be more resistant to the effects of Fes1 oxidation, as Fes1 inhibition required more oxidant (20-fold molar excess NaOCl) compared with other Hsp70 activity assays, where Fes1 inhibition was observed upon oxidation with 10-fold molar excess NaOCl (Fig. 4, *B–D*). It is unclear whether the increased oxidant requirement we observed relates to technical differences for the distinct assays or whether the necessity for additional oxidation to impact peptide release has biological implications.

Most recently, a new activity for the N-terminal region of Fes1 as a pseudo-peptide has been reported, wherein the association of the Fes1 N terminus with the substrate-binding domain prevents the re-association of released peptide with the Hsp70, to further facilitate Hsp70 peptide clearance (Fig. 4*A*) (26). Fes1 was found to limit association of a dansyl-labeled NR peptide with Ssa1, and this activity of Fes1 depended on the presence of an intact Fes1 N terminus (26). Using anisotropy, we observed a similar decrease in the association of Ssa1 with a 6-carboxyfluorescein (FAM)-labeled NR peptide in the presence of Fes1 (Fig. 4*G*). We found that oxidant-treated Fes1 was less effective in limiting peptide association (Fig. 4*G*). Altogether, these data suggest that oxidation diminishes all known Hsp70-associated Fes1 activities; oxidation decreases the ability of Fes1 to facilitate Hsp70 nucleotide exchange, mediate peptide release, and limit peptide association.

### *Interaction between Fes1 and Hsp70 is diminished upon Fes1 oxidation*

Structural data for the Fes1 ortholog HspBP1 shows that the core domain adopts a largely α-helical structure with a concave face that embraces lobe II of the Hsp70 NBD (25). Four helical repeats (formed by helices 3–14) adopt a structure similar to Armadillo repeats; these repeats are capped at each end by longer helices (α1 and α15–17) (25). Homology modeling based on the HspBP1 core structure predicts that the oxidant-sensitive methionines for Fes1 map along α1 (Fig. S1) (22). It has been suggested that a steric clash between α1 and the Hsp70 NBD is what propels the change in NBD conformation that facilitates nucleotide exchange (25). We reasoned that oxidized Fes1 (when associated with Hsp70) may be unable to facilitate a change in NBD conformation (and nucleotide release). Alternatively, we speculated that conformational changes with α1 induced by oxidation may serve to more globally disrupt the core domain structure and alter the ability for major contacts to form between the Hsp70 lobe II and the Armadillo repeats, precluding the association of Hsp70 and Fes1.

To test the latter possibility, we examined whether the association of Fes1 and Hsp70 was altered upon oxidation. Purified recombinant $His_6$-tagged Fes1 was immobilized on Ni-NTA resin after treatment with oxidant (or mock treatment). Immobilized Fes1 was then incubated with an equimolar amount of untagged recombinant Ssb1. Yeast-purified Ssa1 preparations could not be used in this assay, as Ssa1 was tagged with a $His_6$-tag. Consistent with prior studies, we observed a stable association of Fes1 with Ssb1 (Fig. 5*A*) (22). We found that the interaction between Fes1 and Hsp70 was diminished upon Fes1 oxidation (Fig. 5*A*). The decreased interaction correlated with the degree of Fes1 oxidation; treatment of Fes1 with increasing amounts of NaOCl corresponded with the appearance of increasingly-slower migrating Fes1 species and a decrease in Hsp70 association (Fig. 5*A*). A modest background binding of Ssb1 with the Ni-NTA beads was observed even in the absence of Fes1 protein (Fig. 5*A*, *lane 7*); however, the majority of recovered Ssb1 signal in the pulldowns required the presence of Fes1. The decreased association between oxidized Fes1 and Ssb1 could be reversed by Mxr1/2 treatment; the recovery of Hsp70 bound to immobilized Fes1 was increased in samples where oxidant-treated Fes1 was incubated with Mxr1/2 prior to immobilization (Fig. 5*B*, *lanes 6 versus 5*). The presence of Mxr1/2 and the thioredoxin system alone did not alter the association of unmodified Fes1 and Ssb1 (Fig. 5*B*, *lanes 3* and *4*).

Similar results were obtained also for experiments wherein a more complex mixture of yeast cell lysate was used in lieu of purified Hsp70 protein. Cytoplasmic Hsp70s of both the Ssa and Ssb class were isolated from yeast lysates by immobilized FLAG-tagged Fes1 (Fig. 5*C*), similar to what has been reported previously (21, 22). Treatment of Fes1–FLAG with oxidant prior to immobilization decreased the recovery of Ssa–Fes1 and Ssb–Fes1 complexes (Fig. 5*C*). A striking protein band of ~70 kDa was isolated in complex with untreated (reduced) Fes1, and recovery of this band decreased upon Fes1 oxidation (Fig. 5*C*). The ~70-kDa band was confirmed to include both Ssa and Ssb proteins by Western blotting (Fig. 5*C*). We noted above that similar to oxidized Fes1, a Met–to–Gln mutant shows altered NEF activity (Fig. S3). We observed that recovery of both Ssa and Ssb proteins was decreased also for a FLAG-tagged Fes1 Met–to–Gln mutant (Fig. 5*D*), relative to untreated (reduced) WT Fes1–FLAG. Altogether, these data suggest that Fes1 oxidation disrupts the interaction with Hsp70. A decreased association between Hsp70 and Fes1 upon oxidation is consistent with the overall disruption of Fes1 activities, including the ability to facilitate nucleotide exchange, peptide binding, and peptide clearance (Fig. 4).

## Discussion

We identified the yeast cytoplasmic NEF Fes1 as prone to methionine oxidation under excessively-oxidizing conditions. Our data show that when a cluster of three methionines (Met-45, Met-49, and Met-53) in the Fes1 core domain are oxidized, the physical association of the cytoplasmic Hsp70s and Fes1 is diminished (Fig. 5), which correlates with an observed decrease in the ability of oxidized Fes1 to stimulate Hsp70 nucleotide exchange, peptide release, and/or peptide association (Fig. 4). Although the impact for Fes1 oxidation on yeast physiology remains a focus for future research efforts in the lab, we speculate that altered activity of Fes1 upon oxidation may benefit cells during oxidative stress by helping to maintain cytoplasmic proteostasis (53).

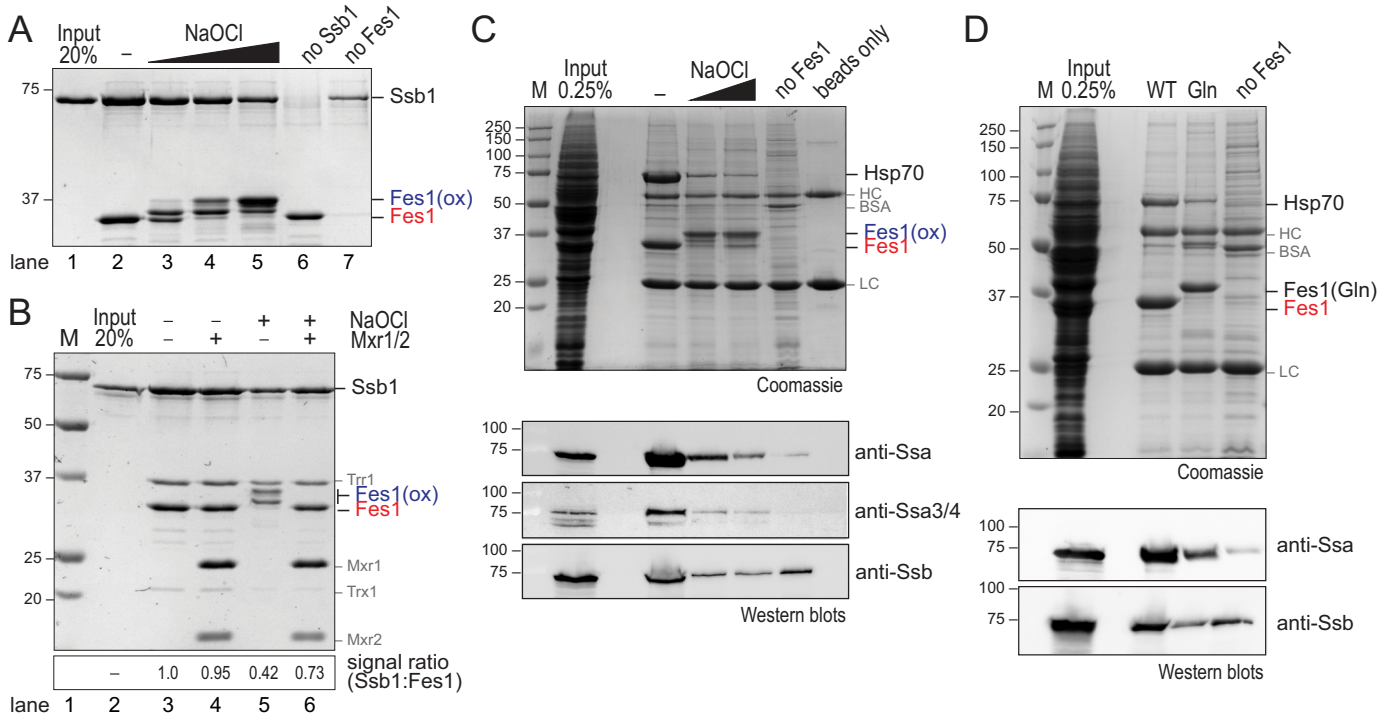


**Figure 5. Fes1 and Hsp70 association is diminished upon Fes1 oxidation.** *A*, purified recombinant Fes1–$His_6$ was oxidized with increasing concentrations of NaOCl (0–20-fold molar excess), desalted, and bound to Ni-agarose beads. Bound Fes1 was incubated with a 2-fold molar excess of Ssb1 for 1 h, and material associated with Fes1 was collected by centrifugation, eluted from the beads with SDS, resolved by reducing SDS-PAGE, and visualized by staining with Coomassie Brilliant Blue. *B*, purified recombinant Fes1–$His_6$ was treated with NaOCl, desalted, and incubated (or mock-treated) with equimolar Mxr1 and Mxr2 proteins for 30 min prior to binding Fes1 to Ni-agarose beads. Binding of Ssb1 was assessed as in *A*. The ratio of Ssb1 bound was quantified based on band intensity, which was quantified and normalized to the unmodified Fes1 control. Data in *A* and *B* depict representative images from at least three independent experiments. *C* and *D*, Fes1–FLAG proteins (WT or a Met–to–Gln mutant) were bound to anti-FLAG beads. *C*, purified recombinant Fes1–FLAG was oxidized with increasing concentrations of NaOCl (10- or 20-fold molar excess) and subsequently desalted prior to mixing with anti-FLAG beads. Bound Fes1 proteins were incubated with WT yeast cell lysates for 2 h, and the material associated with Fes1 was collected by centrifugation and eluted from the beads with SDS. Eluted protein samples were resolved by reducing SDS-PAGE and visualized by staining with Coomassie Brilliant Blue or by Western blotting with the indicated anti-Hsp70 antibodies. *HC*, heavy chain; *LC*, light chain from anti-FLAG beads. Data in *C* and *D* depict representative images from a minimum of two independent experiments.

A variety of proteins post-translationally modified by MetO have been identified from a range of species, including many proteins identified as oxidized in proteome-wide studies of human cells treated with various oxidants (9, 12, 54, 55). Recently, a database (MetOSite) was constructed, which catalogs MetO sites from 3562 different proteins identified across 23 species (56). Notably few *S. cerevisiae* methionine oxidation–susceptible proteins are annotated in the MetOSite, and our identification of Fes1 further extends the known targets of MetO oxidation in this widely-studied model organism. MetOSite lists only two yeast proteins identified as susceptible to methionine oxidation: Mge1 (41) and enolase (shown to be oxidized *in vitro*) (12).

Interestingly, one of the two reported yeast proteins susceptible to oxidation (Mge1) is a NEF for the mitochondrial Hsp70s, and it is attractive to consider that changes to Hsp70 chaperone function through modulation of NEF activity could be a common theme in the response to oxidative stress in the mitochondria and cytoplasm of yeast. The human orthologs of the Hsp70 NEFs Fes1 (HspBP1) (54, 55), Mge1 (GrpEL) (54, 57), and the cytoplasmic BAG family (54, 55) have also been identified with MetO adducts in proteomic studies, and we further speculate that modulation of Hsp70 activity through NEF oxidation may be conserved across species. Similar to what we report for Fes1, directed studies of yeast Mge1 have demonstrated that methionine oxidation lessens the interaction between Mge1 and Hsp70 and decreases Mge1 NEF activity (41, 58, 59). *In vitro* oxidation of GrpEL similarly was shown to lessen the ability of GrpEL to stimulate Hsp70 ATPase activity (58).

We propose that a decrease in Fes1 activity upon oxidation may be of benefit to cells during oxidative stress. A global inactivation of cellular NEF activity during oxidative stress could result in a prolonged association of ADP-bound Hsp70 with peptide, which could serve to limit protein aggregation during overly-oxidizing conditions. However, cells contain multiple NEFs from distinct structural families (GrpE, Hsp110, Fes1, and BAG family proteins) (13), and not all cellular NEF proteins have been identified as prone to oxidation. In addition, for the subset of NEFs identified as susceptible to MetO oxidation in prior proteomic studies (mammalian HspBP1, GrpEL, and BAG proteins), only GrpEL has been shown to become inactivated upon methionine oxidation (58). Thus, we find it interesting to consider specifically how inactivation of Fes1 activity might benefit cells.

It has been previously shown that a strain disrupted for Fes1 activity (a *fes1*Δ) displays a decreased translation rate (35) and a constitutively up-regulated heat-shock response (21). Given that oxidation inactivates Fes1 activity (as would be true for a *fes1*Δ), we speculate that Fes1 MetO modification could acti-

vate beneficial stress responses such as translation attenuation or the HSR, which would help cells cope with excess ROS during oxidative stress. Ssb1/2 have an established role in protein translation (60), and consistent with a change in translation upon Fes1 oxidation, we found Fes1 oxidation lessened the association of Fes1 with Ssb1/2 (Fig. 5). It has been suggested that Fes1 may help to unload (release) the nascent chain from Ssb1 (22), and a loss of Fes1 activity could slow translation by stalling the nascent chain release. A decrease in protein load during unfavorable folding conditions could benefit cells by decreasing the folding burden on an already stressed cytoplasmic system. We also observed an elevated HSR for cells containing a Fes1 Met–to–Gln mutant (Fig. 1). Similar functional outcomes have been reported for proteins with methionine(s) modified with methionine sulfoxide or mutagenized to glutamine (37, 38). Consistent with the behavior of the Fes1 Met–to–Gln substitutions as oxidomimetics, we observed that oxidized Fes1 and a Fes1 Met–to–Gln mutant both showed a decrease in NEF activity (Fig. 4 and Fig. S3) and a lessened association with Hsp70 (Fig. 5). We suggest that the elevated HSR seen for the Fes1 Met–to–Gln allele would be consistent with HSR up-regulation as a consequence of Fes1 methionine oxidation. We speculate that an increased production of HSR targets (including additional chaperones) could serve to buffer against an unfavorable folding environment during excessively-oxidizing conditions.

Moreover, the recently reported role for the Fes1 N-terminal region in peptide clearance suggests a unique activity for Fes1, relative to the other classes of cytoplasmic NEFs (Hsp110 and BAG proteins) that may be modulated by oxidation (26). It was reported that the unstructured Fes1 N-terminal domain associates with the Hsp70 SBD to limit Hsp70 re-association of aggregation-prone substrates; aggregation-prone substrates are proposed to include substrates with multiple exposed hydrophobic patches that possess low apparent Hsp70 off-rates (26). We suggest that during oxidative stress, the chance for productive folding is low. We hypothesize that Fes1 inactivation during these suboptimal folding conditions would prolong the interaction of substrates with the cytoplasmic Hsp70s, due to the continued re-association of released substrates in the absence of the action of the Fes1 N terminus. We propose this extended Hsp70 binding may serve to limit the release and subsequent aggregation of aggregation-prone substrates. It is inferred that substrates prevented from re-associating with Hsp70 (due to normal Fes1 activity) are delivered to the proteasome to be degraded (26), and it is interesting to consider why cells under oxidative stress might prioritize prolonged Hsp70 – substrate interaction over substrate degradation. We propose that an extended Hsp70 association of aggregation-prone substrates during oxidative stress may be advantageous due to the compromised activity of the 26S proteasome and ubiquitination-activating/conjugation machinery during oxidative stress (61).

Alternatively (but not mutually exclusively), a decreased association of oxidized Fes1 with the cellular Hsp70s may promote the interaction of Hsp70 chaperones with other binding partners that in turn act to beneficially modulate Hsp70 chaperone activity. In mammals, HspBP1–Hsp70 complex formation precludes the association of Hsp70 with the ubiquitin ligase CHIP (62), and HspBP1–Hsp70 association has been shown to interfere with CHIP-induced degradation of misfolded Hsp70 substrates, including the cystic fibrosis transmembrane regulator (CFTR) and sequestered antigens (62–64). Although yeast do not contain a CHIP homolog, it is tempting to speculate that additional Hsp70 interactors exist that may complex with Hsp70 in the absence of Fes1 to alter Hsp70 chaperone function during oxidative stress. In mammals, we speculate that oxidation of HspBP1 could promote the association of Hsp70 with CHIP to facilitate protein turnover.

How oxidation of Met-45, Met-49, and Met-53 disrupts Hsp70 association (and decreases Fes1 activity) remains to be determined. For the structurally distinct NEF Mge1 (65), oxidation was demonstrated to disrupt dimer formation (59), and it was speculated that the dissociation of Mge1 dimers accounts for the concomitant decrease in Hsp70 association (59). Given the monomeric structure of HspBP1 (25), we anticipate that Fes1 oxidation disrupts Hsp70 association through a different means. Based on homology modeling, we suggest that all three Fes1 methionines localize to one face of the first helix ($\alpha$1) in the Fes1 core domain (Fig. S1). Physical contact between the Hsp70 NBD and the analogous $\alpha$1 helix of human HspBP1 or the yeast ER ortholog Sil1 was not observed in the published Hsp70 –NEF complex structures (25, 66). Thus, we do not expect Fes1 oxidation to disrupt an Hsp70 –NEF interface. Yet, both structures were solved for only a portion of the NEF (the core domain), and it remains possible that the $\alpha$1 helix forms direct Hsp70 contacts that remain to be observed and that may be altered upon NEF oxidation. We can envision also that oxidation of methionines in $\alpha$1 may perturb the structure of helix 1, which could limit Hsp70 association as a consequence of concomitant changes to the positioning of the flanking N-terminal region and/or to the conformation of the Fes1 core. Helix destabilization would be consistent with other reported examples of the outcome for methionine oxidation; for example, a loss of the secondary helical structure as a consequence of methionine sulfoxide formation was shown to disrupt interactions normally formed by the $\beta$-amyloid peptide and small heat-shock proteins (67, 68). Similar to what we observed for Fes1, methionine residues within and around the $\alpha$1 helix of human HspBP1 (Met-93 and -104) have been identified as susceptible to oxidation (9, 54, 55). Despite an overall poor primary sequence homology between yeast Fes1 and human HspBP1 (Fig. S1), we speculate that oxidation may occur at structurally analogous positions and serve to similarly impact NEF activity. Although our understanding of the exact nature of MetO-induced structural perturbations in Fes1 remains imprecise, it is evident that altering the oxidant-susceptible methionine residues in the $\alpha$1 region perturbs Fes1 function; all of the site-directed mutations we generated at these residues resulted in proteins with compromised activity (Fig. S3).

Our characterization of Fes1 oxidation also revealed a cytoplasmic pool of the methionine sulfoxide reductase enzyme Mxr2 (Fig. 3), which was characterized previously as a mitochondrial enzyme (40). Our data establish Fes1 as the first substrate of cytoplasmic Mxr2 activity (Fig. 3); Mge1 has been characterized as a mitochondrial Mxr2 substrate (41). To the

best of our knowledge, our data characterize Fes1 also as the first substrate of yeast Mxr1.

Uncovering a pool of cytoplasmic Mxr2 begins to explain how reversible methionine oxidation is achieved for cytoplasmic yeast proteins. It is anticipated that oxidation of proteins results in a mixture of both *S*-MetO and *R*-MetO adducts. A MetO epimerase enzyme (capable of interconverting *S*- and *R*-MetO species) has not been identified in yeast (or any other organism), and until now the cytoplasm was expected to contain a single enzyme with select activity toward *S*-MetO (40). A cytosolic pool of both Mxr1 and Mxr2 explains how yeast can reduce cytoplasmic proteins modified by both *S*-MetO and *R*-MetO. The efficient reduction of MetO adducts allows cells to regulate signaling events brought about by MetO protein modifications and also limits the overoxidation of methionine sulfoxide residues to irreversible methionine sulfone species, which may lead to protein aggregation and damage. Although identification of two cytoplasmic Msrs begins to clarify how reversible methionine oxidation is achieved in the yeast cytosol, we speculate that other yeast Msr proteins likely remain to be identified, including a mitochondrial enzyme with activity toward *S*-MetO as well as enzymes localized to the nucleus or endoplasmic reticulum. Furthermore, we anticipate that yet to be uncovered mechanisms may exist to regulate the distribution of Mxr2 between the cytoplasm and mitochondria depending on the redox conditions within these organelles.

In conclusion, our data establish a role for reversible methionine oxidation of Fes1 in regulating the interaction between Fes1 and Hsp70 and in modulating Hsp70 activities. Our results provide a new perspective on how activities of the well-studied Hsp70 family can be attuned by ROS and further define how methionine modification is used as a means for cells to sense and respond to oxidative stress. We anticipate that Fes1 MetO modification may be conserved in other species, and we speculate that inactivation of Fes1 via MetO modification may be an important means to regulate the critical activities of Hsp70 chaperones during oxidative stress.

## Experimental procedures

### *Plasmid construction*

A complete list of plasmids can be found in Table S1. Yeast expression plasmids derive from the pRS vector series (69). Gene sequences were amplified from genomic DNA prepared from S288C strains CSY5 or BY4741 (70). For expression from the endogenous promoter elements, sequences coding for the ORF plus ~1 kb and ~500 bp of the 5′ and 3′ UTR, respectively, were amplified. Epitope-tagged versions of Fes1 were constructed by insertion of sequence for a 3×FLAG epitope or GFP immediately prior to the stop codon. Plasmids pEN254–257 were generated by insertion of amplified *MXR1* or *MXR2* sequences plus sequence coding for a C-terminal mNeonGreen tag into a p416TEF vector (53) (ATCC plasmid no. 87368). pEN3 and pEN86 were constructed by cloning the DNA for the complete Fes1 coding sequence or sequence coding for Fes1 residues 38–290 into a pET21b vector (EMD Millipore) to generate an in-frame C-terminal $His_6$-tag. The coding sequences for yeast Mxr1, Mxr2 (beginning at residue 30), Trx1, and Trr1 and were similarly cloned into pET28a (EMD Millipore) to create an in-frame N-terminal $His_6$-tag and to generate plasmids pEN55, pBM1, pEN208, and pEN108. Complete Ssb1 and Fes1 coding sequences were inserted into a modified version of the pET28a vector containing a $His_6$–SUMO tag to construct pEN130 and pEN253. For pEN253, a C-terminal 3×FLAG was inserted immediately prior to the stop codon. To make pEN21, DNA sequence coding for the Ydj1 J-domain (residues 1–69) was inserted into pGEX-5X-3 (GE Healthcare). pCS980 was constructed by inserting the upstream sequence from *SSA3* (nucleotides −468 to +6) prior to the bacterial *lacZ* sequence in a pRS315 vector. QuikChange site-directed mutagenesis (Agilent Technologies) was performed to generate amino acid substitutions. All plasmids and mutations generated were confirmed by sequencing.

### *Yeast strains and growth conditions*

*S. cerevisiae* strains were grown and genetically manipulated using standard techniques (71). Cultures were grown in rich medium (1% Bacto-yeast extract and 2% Bacto-peptone) containing 2% dextrose (YPD) or 2% galactose (YPGal) or minimal medium (0.67% nitrogen base without amino acids supplemented with 14 amino acids, uracil, and adenine) containing 2% dextrose (SMM) or 2% galactose (SGal). Uracil or leucine supplements were removed from minimal media to select for plasmids as needed.

A complete list of yeast strains used in this study can be found in Table S2. Strain CSY751 was made by one-step gene replacement of the coding region of *FES1* with KanMX in BY4741 (72). Strains CSY974-976 were generated from standard crosses initiated from the *mxr1*Δ and *mxr2*Δ BY47411 and BY4742 deletion collection strains (Research Genetics). Strain CSY825 was a kind gift from Dr. Kevin Morano (University of Texas Health Science Center) and is described in Ref. 21. Strain AJMY28 was generously provided by Dr. Jeffrey Brodsky (University of Pittsburgh) and is described in Ref. 73.

### *Cell-based assays to monitor levels of oxidized Fes1 in vivo*

Yeast cells expressing Fes1–FLAG constructs were grown to mid-log phase in minimal medium, and cultures were treated for the final 30 min prior to harvesting at 30 °C with the following stressors: 5–10 mM hydrogen peroxide (EMD), 5–10 mM *tert*-butyl hydroperoxide (Alfa Aesar), 5–10 mM cumene hydroperoxide (CHP) (Alfa Aesar), 0.5–1 mM sodium hypochlorite (Sigma), 10–50 μg/ml, cycloheximide (Amresco), 5–10 mM dithiothreitol (DTT) (GoldBio), or 5–10 mM diamide (TCI). Heat-shocked samples were shifted to a 37 °C water bath for 1 h prior to harvest. Cells (5 $OD_{600}$) were harvested and washed in sterile water, and lysates were prepared by alkaline lysis (74). Proteins were suspended in 100 μl of SDS sample buffer (60 mM Tris-HCl, pH 6.8, 5% glycerol, 2% SDS, 0.0025% bromphenol blue) with 5% BME, and samples were boiled at 100 °C for 5 min. Insoluble material was removed with a 1-min spin at 21,130 × *g*. Soluble proteins were separated by reducing SDS-PAGE (12% gel) and transferred to nitrocellulose. Proteins were detected using an anti-FLAG mouse mAb (Agilent Technologies; catalog no. 200472) or anti-FLAG rat mAb (Thermo Fisher Scientific; clone L5, catalog no. MA1-142), and an Alexa

488–conjugated anti-mouse (Invitrogen; catalog no. A11029) or an Alexa 488- or Alexa 546–conjugated anti-rat (Invitrogen; catalog nos. A11006 and A11081) secondary antibody. Fluorescent signals were detected with a ChemiDoc MP system (Bio-Rad). Images shown are representative of at least three independent experiments.

### *Heat-shock activation assay*

Yeast (CSY825) transformed with an *HSE-lacZ* reporter plasmid (pCS980) and the indicated *CEN FES1* plasmids (pEN139 and pEN141–143) were grown in SMM medium at 30 °C until mid-log phase ($OD_{600}$ between 0.5 and 0.7). Heat-shocked samples were shifted to a 37 °C water bath for the last 1 h prior to harvest. Cells were permeabilized using Y-PER (Thermo Fisher Scientific), and β-gal activity was quantified as described (75). For each experiment, three yeast transformants of each strain were assayed in duplicate. Error bars denote standard deviation of the average from three independent experiments.

### *Mass spectrometry*

WT cells expressing Fes1–FLAG from a 2-μm plasmid were grown in SMM medium at 30 °C until mid-log phase and were treated with 10 mM CHP for 30 min at 30 °C prior to harvest. Cells (200 $OD_{600}$) were collected, washed in sterile water, and lysed by alkaline lysis (74). Proteins were suspended in 100 μl of SDS sample buffer with 5% BME, and samples were boiled at 100 °C for 5 min. Lysate proteins were incubated for 30 min at room temperature in 1 ml of IP buffer (50 mM Tris-HCl, pH 7.4, 150 mM NaCl, 1% Triton X-100). Unbroken cells and insoluble material were removed by centrifugation for 5 min at 21,130 × *g*. The remaining supernatant (1 ml) was added to 250 μl of anti-FLAG bead resin slurry (Sigma) and incubated overnight at 4 °C. Beads were washed five times with 1 ml of IP buffer, and bound proteins were eluted using 250 μl of SDS sample buffer with 5% BME and boiled at 100 °C for 5 min. To concentrate proteins, 1.5 ml of cold acetone was added and incubated at −20 °C overnight. Protein precipitate was collected after a 21,130 × *g* spin at 4 °C for 15 min, dried, and resuspended in 40 μl of SDS sample buffer with 5% BME. Proteins were separated by reducing SDS-PAGE (10% gel) and visualized with SYPRO Ruby (Invitrogen). Gel bands corresponding to Fes1–FLAG were extracted and analyzed by MS at the Cornell University Proteomics and Mass Spectrometry Core facility. To limit spontaneous methionine oxidation, all sample preparation steps at the facility were conducted in the presence of 20 mM methionine, and trypsin digestion was limited to 3 h at room temperature, and the HPLC trapping column was pre-washed with 20 mM EDTA three times prior to nanoLC-MS/MS analysis.

### *Protein expression and purification*

Plasmids encoding for recombinant $His_6$-tagged proteins (Fes1, Mxr1, Mxr2, Trx1, and Trr1) were transformed into BL21 (DE3) cells, and fresh transformants were grown overnight at 37 °C in LB medium containing 100 μg/ml ampicillin or 15 μg/ml kanamycin. The following morning, cells were diluted 1:50 into LB containing fresh antibiotic, and cultures were grown at 37 °C until an $OD_{600}$ of 0.5 was reached. Cells were shifted to 18 °C for 30 min, and protein expression was induced with 0.5 mM isopropyl β-D-thiogalactopyranoside (GoldBio). After 18 h, cells were harvested, and pellets were stored at −80 °C. Cells were thawed and resuspended in lysis buffer (50 mM sodium phosphate, pH 8, 0.5 M NaCl, 10 mM imidazole, 10% glycerol) containing an EDTA-free protease inhibitor mixture (Pierce), 5 mM BME, 12.5 units/ml benzonase (Pierce), and 2 mg/ml lysozyme (VWR). Resuspended cells were lysed on ice with a microtip sonicator using five 30-s pulses (with a 2-min rest between pulses) at a 60% duty cycle. Insoluble material was removed by centrifugation at 23,700 × *g* for 20 min at 4 °C. Soluble material was loaded onto a HiTrap chelating column (GE Healthcare) charged with nickel. The column was washed with at least 10 column volumes (cv) of lysis buffer and 10 cv of wash buffer (50 mM sodium phosphate, pH 8, 0.5 M NaCl, 20 mM imidazole, 10% glycerol) until the $A_{280}$ signal baselined. Protein was eluted with 5 cv of elution buffer (50 mM sodium phosphate, pH 8, 0.5 M NaCl, 250 mM imidazole, 10% glycerol). Protein fractions were collected, exchanged into desalting buffer (10 mM Tris-HCl, pH 7.4, 50 mM NaCl, 10% glycerol) using a PD-10 desalting column (GE Healthcare), and concentrated using a centrifugal filter (Millipore). Purified proteins were flash-frozen in liquid nitrogen and stored at −80 °C. Concentrations were determined by BCA protein assay (Thermo Fisher Scientific) using BSA as a standard.

$His_6$–SUMO–Ssb1 (pEN130) and $His_6$–SUMO–Fes1–FLAG proteins (pEN253 and pEN258) were expressed and purified by metal-affinity chromatography as above. Protein elution fractions were collected and concentrated, and the $His_6$–SUMO tag was cleaved off the protein at 4 °C using recombinant yeast $His_6$–Ulp1 protease. Proteins were exchanged into lysis buffer with a PD-10 column (to remove imidazole), and the uncleaved protein, protease ($His_6$-tagged), and the released $His_6$–SUMO tag were removed with a HiTrap chelating column charged with nickel and equilibrated in lysis buffer. Fes1–FLAG was used without additional purification. Untagged Ssb1 was further purified to facilitate nucleotide removal. Ssb1 protein fractions were exchanged into 10 mM Tris-HCl, pH 7.4, 10% glycerol, 10 mM EDTA using a PD-10 desalting column and incubated at 4 °C overnight to allow for nucleotide release. Apoprotein was isolated using a HiTrap Blue HP column (GE Healthcare). Ssb1 was eluted with a salt gradient (0–2 M NaCl), and fractions containing Ssb1 were collected and concentrated, and Ssb1 protein was stored in desalting buffer (10 mM Tris-HCl, pH 7.4, 50 mM NaCl, 10% glycerol) at −80 °C. Purified protein was confirmed to be nucleotide-free by HPLC.

Plasmid coding for GST–Ydj1(1–69) (pEN21) was similarly transformed into BL21 (DE3) cells, and protein was expressed as above. Harvested cells were thawed and resuspended in PBS containing an EDTA-free protease inhibitor mixture, 5 mM BME, 12.5 units/ml benzonase, and 2 mg/ml lysozyme and lysed by sonication as above. After sonication, 0.1% Triton X-100 final was added to the lysate mixture. Insoluble material was removed by centrifugation at 23,700 × *g* for 20 min at 4 °C, and soluble material was loaded onto a GSTrap column (GE Healthcare). The column was washed with at least 20 cv of wash buffer 1 (PBS with 2 mM EDTA), 20 cv of wash buffer 2 (PBS

with 2 mM EDTA, 1 M KCl, and 0.1% Triton X-100), 20 cv of ATPase wash buffer (50 mM Tris-HCl, pH 7.4, 2 mM ATP, 10 mM $MgOAc_2$, 200 mM KOAc), and 10 cv of PBS until the $A_{280}$ signal of the column flow-through baselined. Protein was eluted with 5 cv of elution buffer (50 mM Tris-HCl, pH 8, 10 mM reduced GSH, 10% glycerol). Protein fractions were collected, desalted, concentrated, flash-frozen, and stored as above.

The yeast strain AJMY28 was generously provided by Dr. Jeffrey Brodsky (University of Pittsburgh), and $His_6$–Ssa1 was purified from this strain as described previously (73), with minor alterations. Cells freshly streaked from a frozen glycerol stock were grown in SGal-ura medium at 30 °C to saturation. Saturated cultures were diluted 1:20 into YPGal, and cultures were grown overnight (~20 h) at 30 °C until cells reached late log phase ($OD_{600}$ between 2.5 and 3). Cell pellets were harvested and resuspended at a 1:1 volume ratio in Ssa1 lysis buffer (50 mM sodium phosphate, pH 7.8, 300 mM NaCl, 10 mM imidazole, 5 mM BME) containing 1 mM PMSF (VWR) and 1 μM pepstatin A (Alfa Aesar). Suspended cells were frozen by dropwise addition of the cell slurry into liquid nitrogen, and frozen cells were stored at −80 °C. Cells were lysed with 10 2-min runs/1-min rests in a cryomill (SPEX SamplePrep) set at 12 cps. Insoluble material was removed by centrifugation at 23,700 × *g* for 20 min at 4 °C, and soluble material was incubated with Ni-NTA–agarose resin (Thermo Fisher Scientific) for 2 h at 4 °C. The resin was washed with 10 cv of Ssa1 lysis buffer, and bound protein was eluted with 3 cv of Ssa1 elution buffer (50 mM sodium phosphate, pH 7.8, 300 mM NaCl, 200 mM imidazole, 5 mM BME). Ssa1 protein fractions were subsequently diluted with an equal volume of ATP-agarose buffer (25 mM HEPES-KOH, pH 7.4, 10 mM NaCl, 10 mM KCl, 5 mM $MgCl_2$, 2.5% glycerol, 5 mM BME) and loaded onto a 5-ml ATP-agarose column (Sigma, catalog no. A2767). The column was washed with 5 cv of ATP-agarose buffer and then with 5 cv of ATP-agarose buffer with 50 mM NaCl. Bound protein was eluted from the column with 3 cv of ATP-agarose buffer containing 2 mM ATP. Final eluted fractions were collected, exchanged into desalting buffer (10 mM HEPES-KOH, pH 7.4, 50 mM NaCl, 10% glycerol), and concentrated using a centrifugal filter (Millipore). Purified proteins were flash-frozen in liquid nitrogen and stored at −80 °C. Concentrations were determined by a BCA protein assay as above.

### *In vitro Fes1 oxidation and reduction*

Purified recombinant Fes1–$His_6$ protein (10 μM) was diluted in desalting buffer (10 mM Tris-HCl, pH 7.4, 50 mM NaCl) with sodium hypochlorite (Sigma) in quantities ranging from equimolar (10 μM NaOCl) to 20-fold molar excess (200 μM NaOCl) for 60 min at room temperature. To monitor the extent of oxidation, proteins were separated by reducing SDS-PAGE (12% gel) and visualized by staining with Coomassie Brilliant Blue.

To prepare oxidized Fes1 for later reduction with methionine sulfoxide reductase enzymes, Fes1–$His_6$ (50 μM) was incubated with 500 μM NaOCl in desalting buffer for 60 min at room temperature, and excess oxidant was removed with a Bio-Gel P6 Microspin column (Bio-Rad). For all Hsp70 assays making use of oxidant-treated Fes1, buffer with oxidant was similarly desalted for the no Fes1 control. To reduce Fes1 and recycle the Mxr enzymes, oxidized Fes1–$His_6$ (5 μM) was added to $His_6$–Mxr1 (0.5 μM), $His_6$–Mxr2(Δ1–29) (0.5 μM), and either 0.5 mM DTT or a mixture of 0.25 μM $His_6$–Trx1, 0.25 μM $His_6$–Trr1, and 0.5 mM NADPH in a final reaction volume of 50 μl. For Hsp70 assays, oxidized Fes1 was reduced by incubation with equimolar $His_6$–Mxr1 and $His_6$–Mxr2(Δ1–29) in the presence of 10 mM DTT. Samples were incubated with Mxrs for 60 min at room temperature. When analyzed by electrophoresis, samples were quenched with the addition of SDS sample buffer, and proteins were separated by reducing SDS-PAGE (12% gel) and visualized by staining with Coomassie Brilliant Blue.

### *ATP-hydrolysis measurements*

ATP hydrolysis was measured using a modified version of the EnzChek Phosphate Assay kit (Thermo Fisher Scientific) as described previously (76). In brief, ATP hydrolysis was assayed in ATPase buffer (50 mM Tris-HCl, pH 7.4, 50 mM KCl, 5 mM $MgCl_2$, 1 mM DTT) containing 200 μM 2-amino-6-mercapto-7-methylpurine riboside, 0.2 units/ml purine nucleoside phosphorylase, and 5 mM ATP. Phosphate generation was monitored by following the change in absorbance at room temperature using a BioTek Synergy 2 microplate reader. Final protein concentrations were as follows: 0.5 μM $His_6$–Ssa1, 1 μM GST–Ydj1(1–69), and 1 μM Fes1–$His_6$ (reduced or oxidized with 10-fold molar excess NaOCl). Fes1–$His_6$ or GST–Ydj1 proteins were assayed alone to confirm an absence of contaminating ATP hydrolysis activity.

### *Stopped-flow nucleotide and peptide release assays*

Experiments were carried out in HKM buffer (25 mM HEPES-KOH, pH 7.4, 150 mM KCl, 5 mM $MgCl_2$, 1 mM DTT), and data were collected with a Hi-Tech SFA-20 stopped-flow coupled to a Fluoromax-4 spectrofluorometer. To monitor nucleotide release, Ssb1–MABA-ADP complexes were prepared by incubation of 2 μM nucleotide-free Ssb1 and 2 μM MABA-ADP (Jena Bioscience) in a final volume of 2 ml at room temperature for 5 min. Dissociation of the fluorescent nucleotide analog was monitored upon addition of Fes1–$His_6$ and an excess ADP, for a final reaction of 1 μM Ssb1, 1 μM MABA-ADP, 125 μM ADP, and 1 μM Fes1–$His_6$ (reduced or oxidized with 10-fold molar excess NaOCl). Data were collected at 0.05-s intervals during a 60-s time course, with an excitation wavelength of 335 nm, an emission wavelength of 440 nm, and a 3-nm slit width. To monitor peptide release, $His_6$–Ssa1–NBD–NR complexes were prepared by incubation of 5 μM $His_6$–Ssa1 and 2 μM NBD–NRLLLTG peptide (NBD–NR; Elim Biopharmaceuticals) in a final volume of 2 ml at room temperature for 1 h. Dissociation of the fluorescently-labeled peptide was monitored upon addition of excess unlabeled NR peptide (Elim Biopharmaceuticals), ATP, and 5 μM Fes1–$His_6$ (reduced or oxidized with 20-fold molar excess NaOCl). The final reaction consisted of 2.5 μM $His_6$–Ssa1, 1 μM NBD–NR, 250 μM ATP, 125 μM NR peptide, and 2.5 μM Fes1–$His_6$. Data were collected at 0.05-s intervals during a 60-s time course, with an excitation wavelength of 465 nm, an emission wavelength of 533 nm, and a 5-nm slit width. Data curves for nucleotide and

peptide release assays were fit to a one-phase exponential decay using GraphPad Prism (version 8.0).

### *Peptide-association measurements*

Experiments were carried out in HKM buffer, and anisotropy measurements were performed with a Fluoromax-4 spectrofluorometer using a sub-micro quartz fluorometer cell (Starna). Ssa1–Fes1 complex was prepared by incubation of 50 $\mu$M $His_6$–Ssa1 with an equimolar concentration of Fes1–$His_6$ (reduced or oxidized with 10-fold molar excess NaOCl) in a final volume of 50 $\mu$l at room temperature for 30 min. Fluorescently-labeled peptide association was monitored upon addition of a 10 $\mu$M complex to a reaction containing 50 nM fluorescein-labeled NR peptide (FAM–NR; Elim Biopharmaceuticals) in a 150-$\mu$l final volume. Fluorescence anisotropy measurements were collected at 12-s intervals over 60 min at an excitation wavelength of 492 nm, an emission wavelength of 516 nm, and a 12-nm slit width.

### *Cellular subfractionation*

WT yeast cells expressing GFP-tagged Mxr constructs were grown to mid-log phase in minimal medium. Cells (100 $OD_{600}$) were harvested, washed with sterile water, and washed with a buffer of 50 mM Tris-HCl, pH 7.4, 10 mM sodium azide. Cells were incubated in 100 mM Tris-$SO_4$, pH 9.4, with 50 mM BME for 15 min at room temperature, and cells were harvested and resuspended in 1.2 M sorbitol with 10 mM Tris-HCl, pH 7.4, plus lyticase. After a 45-min incubation at room temperature, spheroplasts were harvested by centrifugation, washed with 10 mM Tris-HCl, pH 7.4, 1.2 M sorbitol, and lysed on ice using a Dounce homogenizer in 1 ml of lysis buffer (0.2 M sorbitol, 50 mM Tris-HCl, pH 7.4, 1 mM EDTA) containing a yeast Protease Arrest protease inhibitor mixture (G Biosciences). Cell debris was cleared by centrifugation at 3000 × *g* at 4 °C, and mitochondria-containing pellets were collected by centrifugation of the post-nuclear supernatant (500 $\mu$l) at 20,000 × *g* at 4 °C. The mitochondria-containing pellet was resolubilized and saved for further analysis. A portion (250 $\mu$l) of the post-mitochondrial (cytosolic) fraction was re-centrifuged at 70,000 × *g* at 4 °C to remove high-density membranes and protein aggregates, and the remaining soluble material was saved as a representative of the cytosol. SDS sample buffer and 5% BME final were added to proteins collected in each fraction sample, and proteins were separated by reducing SDS-PAGE (12% gel). Proteins were transferred to nitrocellulose, and Mxr proteins were detected using an anti-GFP mouse mAb (Clontech; catalog no. 632569). Control proteins were detected using mouse monoclonal anti-porin (Invitrogen; clone 16G9E6BC4, catalog no. 459500) or anti-Pgk1 (Invitrogen; clone 22C5D8, catalog no. 459250) antibodies. Protein signals were visualized using an Alexa 488–conjugated anti-mouse secondary antibody and a ChemiDoc MP system. A representative image of three independent experiments is shown.

### *Fluorescence microscopy*

Images were acquired using a CSU-X spinning-disk confocal microscopy system (Intelligent Imaging Innovations) equipped with a DMI 6000B microscope (Leica) and a ×100 1.47NA field planarity apochromat objective lens and a scientific complementary metal-oxide-semiconductor (sCMOS) camera (ORCA Flash4.0 V2, Hamamatsu). WT cells transformed with pTB3390 (Mito-RFP) (obtained from Dr. Anthony Bretscher, Cornell University, New York) and the indicated *MXR*-mNeonGreen plasmid were grown to log phase at 30 °C in SMM medium, and cells were harvested, attached to a glass-bottomed dish coated with concanavalin A (EY Laboratories, Inc.), and washed with cell medium. Cells were live-imaged at room temperature. SlideBook 6.0 software was used to operate the microscopy system and analyze the images. Multiplane images to reach the top and bottom of each cell were taken at 0.3-$\mu$m steps (~20–25 total planes) and used to create z-stack maximum projections.

### *Protein pulldown assays*

To assess complex formation between recombinant Fes1 and Ssb1, Fes1–$His_6$ (10 $\mu$g) was incubated with 20 $\mu$l of HisPur Ni-NTA magnetic bead suspension (Thermo Fisher Scientific) in a total volume of 100 $\mu$l of binding buffer (50 mM sodium phosphate, pH 8, 100 mM NaCl, 10 mM imidazole, 0.1% Igepal, 2% glycerol, 1 mM DTT, 1 $\mu$M pepstatin A). Samples were rotated for 1 h at 4 °C, and beads were collected by magnetization. Beads were washed three times with 500 $\mu$l of binding buffer to remove unbound proteins, and washed beads were suspended in a final volume of 100 $\mu$l of binding buffer. Untagged Ssb1 (20 $\mu$g) was added to the beads, and samples were rotated at 4 °C for 1 h. Beads were magnetized and washed three times with 500 $\mu$l of binding buffer. Bound proteins were solubilized in 25 $\mu$l of sample buffer containing 5% BME. Samples were resolved on an SDS-acrylamide gel (12%) and visualized with Coomassie Brilliant Blue. Band intensities were quantified using Image Lab software (version 5.2). A representative image of three independent experiments is shown.

To assess association of recombinant Fes1 with yeast cytosolic proteins, Fes1–FLAG (~40 $\mu$g) or an equivalent amount of BSA (Calbiochem) was incubated with 25 $\mu$l of anti-FLAG bead slurry (Sigma) in a total volume of 200 $\mu$l of desalting buffer. Samples were rotated for 1 h at 4 °C, and beads were collected by centrifugation at 1000 × *g* for 2 min. Beads were washed three times with 500 $\mu$l of binding buffer to remove unbound proteins. Cytosol was prepared from WT yeast (BY4741), which were grown to saturation at 30 °C, harvested by centrifugation, and resuspended in a 1:1 volume ratio of desalting buffer containing 1 $\mu$M pepstatin A and 1 mM PMSF. Cells were lysed using a cryomill (SPEX SamplePrep) using 10 2-min runs (with 1-min rest between cycles) at 12 cps. Insoluble lysate material was removed by centrifugation at 23,700 × *g* for 20 min at 4 °C, and the remaining cytosolic fraction (1 ml) was added to the prepared FLAG beads and incubated for 2 h at 4 °C. Beads were collected by centrifugation at 1000 × *g* for 2 min and washed three times with 500 $\mu$l of binding buffer, and proteins were solubilized in 50 $\mu$l of sample buffer containing 5% BME. Proteins were resolved on an SDS-acrylamide gel (12%) and visualized with Coomassie Brilliant Blue stain or by Western blotting. Primary antibodies against the yeast cytosolic Hsp70s (anti-Ssa, anti-Ssa3/4, and anti-Ssb) were generously provided by Dr. Elizabeth Craig (University of Wisconsin-Madison). Proteins were visualized using an Alexa 488 – conjugated anti-rabbit secondary antibody (Invitrogen; catalog no. A21206)

imaged with a ChemiDoc MP system. A representative image of three independent experiments is shown.

### *Statistical analysis*

Data quantification and statistical analysis, including normalization, calculation of means and error, data fitting, and statistical tests, were conducted using GraphPad Prism (version 8.0).

*Author contributions*—E. E. N. data curation; E. E. N. and C. S. S. formal analysis; E. E. N. writing-original draft; E. E. N. and C. S. S. writing-review and editing; C. S. S. conceptualization; C. S. S. supervision; C. S. S. funding acquisition.

*Acknowledgments—We thank Dr. Sheng Zhang and the Cornell University Proteomics Core for their assistance in MS sample preparation and data analysis. We also acknowledge Dr. Anthony Bretscher and Abigail Miller for their assistance in the fluorescence microscopy experiments and Heather Marsh and Beata Mackenroth for technical support. We are grateful to Drs. Anthony Bretscher, Jeffrey Brodsky, Elizabeth Craig, and Kevin Morano their contributions of reagents in this study.*

## References


1. Schieber, M., and Chandel, N. S. (2014) ROS function in redox signaling and oxidative stress. *Curr. Biol.* **24,** R453–R462 CrossRef Medline
2. Brandes, N., Schmitt, S., and Jakob, U. (2009) Thiol-based redox switches in eukaryotic proteins. *Antioxid. Redox Signal.* **11,** 997–1014 CrossRef Medline
3. Paulsen, C. E., and Carroll, K. S. (2010) Orchestrating redox signaling networks through regulatory cysteine switches. *ACS Chem. Biol.* **5,** 47–62 CrossRef Medline
4. Spadaro, D., Yun, B. W., Spoel, S. H., Chu, C., Wang, Y. Q., and Loake, G. J. (2010) The redox switch: dynamic regulation of protein function by cysteine modifications. *Physiol. Plant.* **138,** 360–371 CrossRef Medline
5. Levine, R. L., Mosoni, L., Berlett, B. S., and Stadtman, E. R. (1996) Methionine residues as endogenous antioxidants in proteins. *Proc. Natl. Acad. Sci. U.S.A.* **93,** 15036–15040 CrossRef Medline
6. Levine, R. L., Moskovitz, J., and Stadtman, E. R. (2000) Oxidation of methionine in proteins: roles in antioxidant defense and cellular regulation. *IUBMB Life* **50,** 301–307 CrossRef Medline
7. Stadtman, E. R., Moskovitz, J., and Levine, R. L. (2003) Oxidation of methionine residues of proteins: biological consequences. *Antioxid. Redox Signal.* **5,** 577–582 CrossRef Medline
8. Schöneich, C. (2005) Methionine oxidation by reactive oxygen species: reaction mechanisms and relevance to Alzheimer's disease. *Biochim. Biophys. Acta* **1703,** 111–119 CrossRef Medline
9. Kim, G., Weiss, S. J., and Levine, R. L. (2014) Methionine oxidation and reduction in proteins. *Biochim. Biophys. Acta* **1840,** 901–905 CrossRef Medline
10. Moskovitz, J. (2005) Methionine sulfoxide reductases: ubiquitous enzymes involved in antioxidant defense, protein regulation, and prevention of aging-associated diseases. *Biochim. Biophys. Acta* **1703,** 213–219 CrossRef Medline
11. Ghesquière, B., and Gevaert, K. (2014) Proteomics methods to study methionine oxidation. *Mass Spectrom. Rev.* **33,** 147–156 CrossRef Medline
12. Lin, S., Yang, X., Jia, S., Weeks, A. M., Hornsby, M., Lee, P. S., Nichiporuk, R. V., Iavarone, A. T., Wells, J. A., Toste, F. D., and Chang, C. J. (2017) Redox-based reagents for chemoselective methionine bioconjugation. *Science* **355,** 597–602 CrossRef Medline
13. Rosenzweig, R., Nillegoda, N. B., Mayer, M. P., and Bukau, B. (2019) The Hsp70 chaperone network. *Nat. Rev. Mol. Cell Biol.* **20,** 665–680 CrossRef Medline
14. Mayer, M. P. (2018) Intra-molecular pathways of allosteric control in Hsp70s. *Philos. Trans. R. Soc. B Biol. Sci.* **373,** 20170183 CrossRef Medline
15. Zuiderweg, E. R., Hightower, L. E., and Gestwicki, J. E. (2017) The remarkable multivalency of the Hsp70 chaperones. *Cell Stress Chaperones* **22,** 173–189 CrossRef Medline
16. Kampinga, H. H., and Craig, E. A. (2010) The HSP70 chaperone machinery: J proteins as drivers of functional specificity. *Nat. Rev. Mol. Cell Biol.* **11,** 579–592 CrossRef Medline
17. Kampinga, H. H., Andreasson, C., Barducci, A., Cheetham, M. E., Cyr, D., Emanuelsson, C., Genevaux, P., Gestwicki, J. E., Goloubinoff, P., Huerta-Cepas, J., Kirstein, J., Liberek, K., Mayer, M. P., Nagata, K., Nillegoda, N. B., *et al.* (2019) Function, evolution, and structure of J-domain proteins. *Cell Stress Chaperones* **24,** 7–15 CrossRef Medline
18. Walsh, P., Bursać, D., Law, Y. C., Cyr, D., and Lithgow, T. (2004) The J-protein family: modulating protein assembly, disassembly and translocation. *EMBO Rep.* **5,** 567–571 CrossRef Medline
19. Bracher, A., and Verghese J. (2015) GrpE, Hsp110/Grp170, HspBP1/Sil1 and BAG domain proteins: nucleotide exchange factors for Hsp70 molecular chaperones. In: *The Networking of Chaperones by Co-chaperones.* (Blatch G., and Edkins A., eds) **vol. 78,** Springer, Cham
20. Brodsky, J. L., and Bracher, A. (2007) Nucleotide exchange factors for Hsp70 molecular chaperones. In: *Networking of Chaperones by Co-Chaperones.* (Blatch G., ed) Springer, New York, NY
21. Abrams, J. L., Verghese, J., Gibney, P. A., and Morano, K. A. (2014) Hierarchical functional specificity of cytosolic heat-shock protein 70 (Hsp70) nucleotide-exchange factors in yeast. *J. Biol. Chem.* **289,** 13155–13167 CrossRef Medline
22. Dragovic, Z., Shomura, Y., Tzvetkov, N., Hartl, F. U., and Bracher, A. (2006) Fes1p acts as a nucleotide-exchange factor for the ribosome-associated molecular chaperone Ssb1p. *Biol. Chem.* **387,** 1593–1600 CrossRef Medline
23. Kabani, M., McLellan, C., Raynes, D. A., Guerriero, V., and Brodsky, J. L. (2002) HspBP1, a homologue of the yeast Fes1 and Sls1 proteins, is an Hsc70 nucleotide-exchange factor. *FEBS Lett.* **531,** 339–342 CrossRef Medline
24. Raviol, H., Sadlish, H., Rodriguez, F., Mayer, M. P., and Bukau, B. (2006) Chaperone network in the yeast cytosol: Hsp110 is revealed as an Hsp70 nucleotide-exchange factor. *EMBO J.* **25,** 2510–2518 CrossRef Medline
25. Shomura, Y., Dragovic, Z., Chang, H. C., Tzvetkov, N., Young, J. C., Brodsky, J. L., Guerriero, V., Hartl, F. U., and Bracher, A. (2005) Regulation of Hsp70 function by HspBP1: structural analysis reveals an alternate mechanism for Hsp70 nucleotide exchange. *Mol. Cell* **17,** 367–379 CrossRef Medline
26. Gowda, N. K. C., Kaimal, J. M., Kityk, R., Daniel, C., Liebau, J., Öhman, M., Mayer, M. P., and Andréasson, C. (2018) Nucleotide exchange factors Fes1 and HspBP1 mimic substrate to release misfolded proteins from Hsp70. *Nat. Struct. Mol. Biol.* **25,** 83–89 CrossRef Medline
27. Evans, M. V., Turton, H. E., Grant, C. M., and Dawes, I. W. (1998) Toxicity of linoleic acid hydroperoxide to *Saccharomyces cerevisiae*: involvement of a respiration-related process for maximal sensitivity and adaptive response. *J. Bacteriol.* **180,** 483–490 Medline
28. Grant, C. M., MacIver, F. H., and Dawes, I. W. (1996) Glutathione is an essential metabolite required for resistance to oxidative stress in the yeast *Saccharomyces cerevisiae*. *Curr. Genet.* **29,** 511–515 CrossRef Medline
29. Le, D. T., Liang, X., Fomenko, D. E., Raza, A. S., Chong, C. K., Carlson, B. A., Hatfield, D. L., and Gladyshev, V. N. (2008) Analysis of methionine/selenomethionine oxidation and methionine sulfoxide reductase function using methionine-rich proteins and antibodies against their oxidized forms. *Biochemistry* **47,** 6685–6694 CrossRef Medline
30. Gennaris, A., Ezraty, B., Henry, C., Agrebi, R., Vergnes, A., Oheix, E., Bos, J., Leverrier, P., Espinosa, L., Szewczyk, J., Vertommen, D., Iranzo, O., Collet, J. F., and Barras, F. (2015) Repairing oxidized proteins in the bacterial envelope using respiratory chain electrons. *Nature* **528,** 409–412 CrossRef Medline
31. Kato, M., Yang, Y. S., Sutter, B. M., Wang, Y., McKnight, S. L., and Tu, B. P. (2019) Redox state controls phase separation of the yeast Ataxin-2 protein via reversible oxidation of its methionine-rich low-complexity domain. *Cell* **177,** 711–721.e8 CrossRef Medline
32. Linde, S., Nielsen, J. H., Hansen, B., and Welinder, B. S. (1990) High-performance liquid chromatography of rat and mouse islet polypeptides: po-

tential risk of oxidation of methionine residues during sample preparation. *J. Chromatogr.* **530,** 29–37 CrossRef Medline
33. Swiderek, K. M., Davis, M. T., and Lee, T. D. (1998) The identification of peptide modifications derived from gel-separated proteins using electrospray triple quadrupole and ion trap analyses. *Electrophoresis* **19,** 989–997 CrossRef Medline
34. Klont, F., Bras, L., Wolters, J. C., Ongay, S., Bischoff, R., Halmos, G. B., and Horvatovich, P. (2018) Assessment of sample preparation bias in mass spectrometry-based proteomics. *Anal. Chem.* **90,** 5405–5413 CrossRef Medline
35. Kabani, M., Beckerich, J.-M., and Brodsky, J. L. (2002) Nucleotide exchange factor for the yeast Hsp70 molecular chaperone Ssa1p. *Mol. Cell. Biol.* **22,** 4677–4689 CrossRef Medline
36. Shaner, L., Sousa, R., and Morano, K. A. (2006) Characterization of Hsp70 binding and nucleotide exchange by the yeast Hsp110 chaperone Sse1. *Biochemistry* **45,** 15075–15084 CrossRef Medline
37. Drazic, A., Miura, H., Peschek, J., Le, Y., Bach, N. C., Kriehuber, T., and Winter, J. (2013) Methionine oxidation activates a transcription factor in response to oxidative stress. *Proc. Natl. Acad. Sci. U.S.A.* **110,** 9493–9498 CrossRef Medline
38. Chin, D., and Means, A. R. (1996) Methionine to glutamine substitutions in the C-terminal domain of calmodulin impair the activation of three protein kinases. *J. Biol. Chem.* **271,** 30465–30471 CrossRef Medline
39. Achilli, C., Ciana, A., and Minetti, G. (2015) The discovery of methionine sulfoxide reductase enzymes: an historical account and future perspectives. *Biofactors* **41,** 135–152 CrossRef Medline
40. Kaya, A., Koc, A., Lee, B. C., Fomenko, D. E., Rederstorff, M., Krol, A., Lescure, A., and Gladyshev, V. N. (2010) Compartmentalization and regulation of mitochondrial function by methionine sulfoxide reductases in yeast. *Biochemistry* **49,** 8618–8625 CrossRef Medline
41. Allu, P. K., Marada, A., Boggula, Y., Karri, S., Krishnamoorthy, T., and Sepuri, N. B. (2015) Methionine sulfoxide reductase 2 reversibly regulates Mge1, a cochaperone of mitochondrial Hsp70, during oxidative stress. *Mol. Biol. Cell* **26,** 406–419 CrossRef Medline
42. Michel, A. M., Fox, G., M Kiran, A., De Bo, C., O'Connor, P. B., Heaphy, S. M., Mullan, J. P., Donohue, C. A., Higgins, D. G., and Baranov, P. V. (2014) GWIPS-viz: development of a ribo-seq genome browser. *Nucleic Acids Res.* **42,** D859–D864 CrossRef Medline
43. Horton, P., Park, K. J., Obayashi, T., Fujita, N., Harada, H., Adams-Collier, C. J., and Nakai, K. (2007) WoLF PSORT: protein localization predictor. *Nucleic Acids Res.* **35,** W585–W587 CrossRef Medline
44. Yogev, O., and Pines, O. (2011) Dual targeting of mitochondrial proteins: mechanism, regulation and function. *Biochim. Biophys. Acta* **1808,** 1012–1020 CrossRef Medline
45. Kim, H. Y., and Gladyshev, V. N. (2004) Methionine sulfoxide reduction in mammals: characterization of methionine-*R*-sulfoxide reductases. *Mol. Biol. Cell* **15,** 1055–1064 CrossRef Medline
46. Theyssen, H., Schuster, H. P., Packschies, L., Bukau, B., and Reinstein, J. (1996) The second step of ATP binding to DnaK induces peptide release. *J. Mol. Biol.* **263,** 657–670 CrossRef Medline
47. Mayer, M., Reinstein, J., and Buchner, J. (2003) Modulation of the ATPase cycle of BiP by peptides and proteins. *J. Mol. Biol.* **330,** 137–144 CrossRef Medline
48. Kominek, J., Marszalek, J., Neuvéglise, C., Craig, E. A., and Williams, B. L. (2013) The complex evolutionary dynamics of Hsp70s: a genomic and functional perspective. *Genome Biol. Evol.* **5,** 2460–2477 CrossRef Medline
49. Kumar, S., and Masison, D. C. (2019) Hsp70-nucleotide-exchange factor (NEF) Fes1 has non-NEF roles in degradation of gluconeogenic enzymes and cell wall integrity. *PLoS Genet.* **15,** e1008219 CrossRef Medline
50. Polier, S., Dragovic, Z., Hartl, F. U., and Bracher, A. (2008) Structural basis for the cooperation of Hsp70 and Hsp110 chaperones in protein folding. *Cell* **133,** 1068–1079 CrossRef Medline
51. Pfund, C., Huang, P., Lopez-Hoyo, N., and Craig, E. A. (2001) Divergent functional properties of the ribosome-associated molecular chaperone Ssb compared with other Hsp70s. *Mol. Biol. Cell* **12,** 3773–3782 CrossRef Medline
52. Needham, P. G., Patel, H. J., Chiosis, G., Thibodeau, P. H., and Brodsky, J. L. (2015) Mutations in the yeast Hsp70, Ssa1, at P417 alter ATP cycling, interdomain coupling, and specific chaperone functions. *J. Mol. Biol.* **427,** 2948–2965 CrossRef Medline
53. Mumberg, D., Müller, R., and Funk, M. (1995) Yeast vectors for the controlled expression of heterologous proteins in different genetic backgrounds. *Gene* **156,** 119–122 CrossRef Medline
54. Ghesquière, B., Jonckheere, V., Colaert, N., Van Durme, J., Timmerman, E., Goethals, M., Schymkowitz, J., Rousseau, F., Vandekerckhove, J., and Gevaert, K. (2011) Redox proteomics of protein-bound methionine oxidation. *Mol. Cell. Proteomics* **10,** M110.006866 CrossRef Medline
55. Walker, E. J., Bettinger, J. Q., Welle, K. A., Hryhorenko, J. R., and Ghaemmaghami, S. (2019) Global analysis of methionine oxidation provides a census of folding stabilities for the human proteome. *Proc. Natl. Acad. Sci. U.S.A.* **116,** 6081–6090 CrossRef Medline
56. Valverde, H., Cantón, F. R., and Aledo, J. C. (2019) MetOSite: an integrated resource for the study of methionine residues sulfoxidation. *Bioinformatics* **35,** 4849–4850 CrossRef Medline
57. Hsieh, Y. J., Chien, K. Y., Yang, I. F., Lee, I. N., Wu, C. C., Huang, T. Y., and Yu, J. S. (2017) Oxidation of protein-bound methionine in Photofrin-photodynamic therapy-treated human tumor cells explored by methionine-containing peptide enrichment and quantitative proteomics approach. *Sci. Rep.* **7,** 1370 CrossRef Medline
58. Allu, P. K., Boggula, Y., Karri, S., Marada, A., Krishnamoorthy, T., and Sepuri, N. B. V. (2018) A conserved R type methionine sulfoxide reductase reverses oxidized GrpEL1/Mge1 to regulate Hsp70 chaperone cycle. *Sci. Rep.* **8,** 2716 CrossRef Medline
59. Marada, A., Allu, P. K., Murari, A., PullaReddy, B., Tammineni, P., Thiriveedi, V. R., Danduprolu, J., and Sepuri, N. B. (2013) Mge1, a nucleotide-exchange factor of Hsp70, acts as an oxidative sensor to regulate mitochondrial Hsp70 function. *Mol. Biol. Cell* **24,** 692–703 CrossRef Medline
60. Peisker, K., Chiabudini, M., and Rospert, S. (2010) The ribosome-bound Hsp70 homolog Ssb of *Saccharomyces cerevisiae*. *Biochim. Biophys. Acta* **1803,** 662–672 CrossRef Medline
61. Davies, K. J. (2001) Degradation of oxidized proteins by the 20S proteasome. *Biochimie* **83,** 301–310 CrossRef Medline
62. Alberti, S., Böhse, K., Arndt, V., Schmitz, A., and Höhfeld, J. (2004) The cochaperone HspBP1 inhibits the CHIP ubiquitin ligase and stimulates the maturation of the cystic fibrosis transmembrane conductance regulator. *Mol. Biol. Cell* **15,** 4003–4010 CrossRef Medline
63. Kettern, N., Rogon, C., Limmer, A., Schild, H., and Höhfeld, J. (2011) The Hsc/Hsp70 co-chaperone network controls antigen aggregation and presentation during maturation of professional antigen presenting cells. *PLoS ONE* **6,** e16398 CrossRef Medline
64. Kunisawa, J., and Shastri, N. (2006) Hsp90$\alpha$ chaperones large C-terminally extended proteolytic intermediates in the MHC class I antigen processing pathway. *Immunity* **24,** 523–534 CrossRef Medline
65. Harrison, C. J., Hayer-Hartl, M., Di Liberto, M., Hartl, F., and Kuriyan, J. (1997) Crystal structure of the nucleotide-exchange factor GrpE bound to the ATPase domain of the molecular chaperone DnaK. *Science* **276,** 431–435 CrossRef Medline
66. Yan, M., Li, J., and Sha, B. (2011) Structural analysis of the Sil1-Bip complex reveals the mechanism for Sil1 to function as a nucleotide-exchange factor. *Biochem. J.* **438,** 447–455 CrossRef Medline
67. Watson, A. A., Fairlie, D. P., and Craik, D. J. (1998) Solution structure of methionine-oxidized amyloid $\beta$-peptide(1–40). Does oxidation affect conformational switching? *Biochemistry* **37,** 12700–12706 CrossRef Medline
68. Härndahl, U., Kokke, B. P., Gustavsson, N., Linse, S., Berggren, K., Tjernеld, F., Boelens, W. C., and Sundby, C. (2001) The chaperone-like activity of a small heat-shock protein is lost after sulfoxidation of conserved methionines in a surface-exposed amphipathic $\alpha$-helix. *Biochim. Biophys. Acta* **1545,** 227–237 CrossRef Medline
69. Sikorski, R. S., and Hieter, P. (1989) A system of shuttle vectors and yeast host strains designed for efficient manipulation of DNA in *Saccharomyces cerevisiae*. *Genetics* **122,** 19–27 Medline
70. Brachmann, C. B., Davies, A., Cost, G. J., Caputo, E., Li, J., Hieter, P., and Boeke, J. D. (1998) Designer deletion strains derived from *Saccharomyces cerevisiae* S288C: a useful set of strains and plasmids for PCR-mediated

gene disruption and other applications. *Yeast* **14,** 115–132 CrossRef Medline
71. Adams, A., Gottschling, D. E., Kaiser, C. A., and Stearns, T. (1997) *Methods in Yeast Genetics: A Cold Spring Harbor Laboratory Course Manual*, Cold Spring Harbor Laboratory Press, Cold Spring Harbor, NY
72. Longtine, M. S., McKenzie, A., 3rd., Demarini, D. J., Shah, N. G., Wach, A., Brachat, A., Philippsen, P., and Pringle, J. R. (1998) Additional modules for versatile and economical PCR-based gene deletion and modification in *Saccharomyces cerevisiae*. *Yeast* **14,** 953–961 CrossRef Medline
73. McClellan, A. J., and Brodsky, J. L. (2000) Mutation of the ATP-binding pocket of SSA1 indicates that a functional interaction between Ssa1p and Ydj1p is required for post-translational translocation into the yeast endoplasmic reticulum. *Genetics* **156,** 501–512 Medline
74. Kushnirov, V. V. (2000) Rapid and reliable protein extraction from yeast. *Yeast* **16,** 857–860 CrossRef Medline
75. Guarente, L. (1983) Yeast promoters and lacZ fusions designed to study expression of cloned genes in yeast. *Methods Enzymol.* **101,** 181–191 CrossRef Medline
76. Siegenthaler, K. D., Pareja, K. A., Wang, J., and Sevier, C. S. (2017) An unexpected role for the yeast nucleotide-exchange factor Sil1 as a reductant acting on the molecular chaperone BiP. *Elife* **6,** e24141 CrossRef Medline